EVIDENCE ACCUMULATION AND THE MOMENT OF RECOGNITION: DISSOCIATING PERCEPTUAL DECISION PROCESSES USING FMRI

by

Elisabeth Jeannette Ploran

BA, Drew University, 2004

Submitted to the Graduate Faculty of

Arts and Sciences in partial fulfillment

of the requirements for the degree of

Master of Science

University of Pittsburgh

2008

UNIVERSITY OF PITTSBURGH

ARTS AND SCIENCES

This thesis was presented

by

Elisabeth Jeannette Ploran

It was defended on

August 7, 2007

and approved by

Julie Fiez, Professor, Dept of Psychology

Erik Reichle, Associate Professor, Dept of Psychology

Tessa Warren, Assistant Professor, Dept of Psychology

Thesis Advisor: Mark Wheeler, Assistant Professor, Dept of Psychology

EVIDENCE ACCUMULATION AND THE MOMENT OF RECOGNITION: DISSOCIATING PERCEPTUAL DECISION PROCESSES USING FMRI

Elisabeth J. Ploran, M.S.

University of Pittsburgh, 2008

Decision making can be conceptualized as the culmination of an integrative process in which evidence supporting different response options accumulates gradually over time. We used functional magnetic resonance imaging (fMRI) to investigate brain activity leading up to and during decisions about perceptual object identity. Pictures were revealed gradually and subjects signaled the time of recognition (T_R) with a button press. We examined the timecourse of T_R-dependent activity to determine how brain regions tracked the timing of recognition. In several occipital regions, activity increased as stimulus information increased, independently of T_R, suggesting a role in lower level sensory processing. In inferior temporal (IT), frontal and parietal regions, a gradual buildup in activity peaking in correspondence with T_R suggested that these regions participated in the accumulation of evidence supporting object identity. In medial frontal cortex, anterior insula/frontal operculum, and thalamus, activity remained near baseline until T_R, suggesting a relation to the moment of recognition or the decision itself. The findings dissociate neural processes that function in concert during perceptual recognition decisions.

PREFACE

Portions of this text can be found in published format under the following citation:

Ploran, E.J., Nelson, S.M., Velanova, K., Donaldson, D.I., Petersen, S.E., and Wheeler, M.E. (2007). “Evidence accumulation and the moment of recognition: dissociating perceptual decision processes using fMRI.” *Journal of Neuroscience. 27(44). 11912-11924.*

TABLE OF CONTENTS

LIST OF TABLES

LIST OF FIGURES

1.0 INTRODUCTION

The ability to select a target among alternatives has been studied extensively through many techniques. Studies of decision-making range from behavioral and neurological observation in humans during complex memory and problem-solving tasks, to the recording of single neurons in macaque monkeys during simple perceptual discrimination tasks, and the development of computational diffusion models that can account for these data. Each of these techniques offers a set of advantages and methodological limitations. The comparison and combination of these techniques creates insight into the potential neural substrates underlying decision-making. The examination of these various techniques also illuminates the types of studies needed to fill in the gaps, making the bridges between the areas smaller and easier to cross. The purpose of the current research is to use the comparison of previous research across disciplines to inform and extend the research trajectory, and to attempt to connect some of the results from both human and monkey research by using a common approach.

Humans make decisions constantly, often without conscious awareness. For example, perceptual recognition is usually an automatic process; object identification can occur within 1000 ms of presentation (Roisson & Pourtois, 2004). Similarly, word identification can occur within 750 ms of presentation, for words up to 6 letters in length and 2 syllables (Frederiksen & Kroll, 1976). However, if the object or word is occluded or incomplete, more calculations among the alternatives must be made before a final recognition decision is selected. Consider what

might happen when you are waiting for a bus to go home. On a clear day, it may be easy to see the route header on the front of the bus, allowing you to recognize it and decide whether or not to step forward on the curb. On a rainy day, drizzle may obscure the route header, limiting your ability to perceive the letters and identify the route. Instead of the fast, easy recognition you made on the clear day, you might pause to gather more information, or *evidence*, towards the correct action. Studying this dynamic process, and specifically its evolution over time, can help build an accurate model of decision-making and related processes like recognition. This model can then be used to determine the potential points of deficiency when impairment occurs.

1.1 BEHAVIORAL RESEARCH

Previous researchers have studied the behavioral manifestation of evidence accumulation under many guises. One such guise is the tip-of-the-tongue (TOT) phenomenon, when a participant is unable to give a direct answer to a question, but has the subjective experience of approaching the answer. This experience may include the ability to state many characteristics of the answer such as first letter (Koriat, A. & Leiblich, I., 1977), number of syllables (Rubin, D.C., 1975), and synonyms or homonyms (Cohen, G. & Faulkner, D., 1986; for review, see Brown, A.S., 1991). These characteristics may act as evidence for the answer; when enough of these characteristics are accessed, the TOT experience leads the participant to believe the answer is close. For example, Maril et al. (2001) used the conjunction of two descriptors to evoke a third item, such as “Goodfellas + director” to evoke “Martin Scorsese”. The participant might be able to remark that the director’s last name begins with an “S” and he also directed “Casino”, but still not be

able to state the director's name explicitly. This sense that the target is on the tip of the tongue is a demonstration of how gradual accumulation of evidence might feel subjectively.

In contrast, other behavioral research suggests that the subjective experience during problem-solving is not necessarily a sense of gradually coming closer to the answer. Instead, studies of problem-solving have illustrated the experience of sudden insight, in which a participant might not have any sense of the answer, but then experiences an instantaneous breakthrough that illuminates the solution. One anecdote of sudden insight is the story of Archimedes, who, while taking a bath, realized that water displacement can be used to measure volume. It is said that he then ran through the streets naked shouting, "Eureka!". Problems that consistently evoke this phenomenon across participants are categorized as "insight problems". Controlled studies in the laboratory have examined the feeling-of-knowing, which assesses the participant's sense that he/she is able to find the solution, and compared standard memory paradigms and non-insight problems (i.e. algebra) to the insight problems. In these studies, participants are shown the item and immediately give a rating to indicate their subjective sense that the solution is available to them. These studies consistently demonstrate that participants cannot accurately predict their ability to find the solution to insight problems, despite being accurate in predicting memory performance and their ability to solve non-insight problems (Metcalfe, J., 1986, 1987).

However, it is also possible that there are underlying differences in the structure of the two tasks that may negate comparison of the results. In the TOT task, the participants are trying to recall a very specific target as specified by the cues given in the task, and the targets are most likely very familiar given their pop culture nature. This gives the participant a wealth of cues to use in order to find the target. In contrast, participants in the feeling-of-knowing

experiment tackle the insight problems on an open path without reference cues to aid in their evidence accumulation towards the target solution. Also, the target solution is not necessarily something the participants have encountered before, whereas the TOT task is eliciting a specific target from memory. The potential incomparability of the cognitive approach in these tasks highlights the need for a simple design that reduces this variation, but still produces the experience of both gradual accumulation and insight.

The absence of a gradual growth towards a decision in the feeling-of-knowing studies suggests that perhaps not all decisions are computed the same way, and therefore different neural populations might be responsible for the contrasting experiences. Also, the two tasks are cognitively complex enough that different participants might utilize different approaches even within one task structure. For example, in the TOT task one participant might focus on the word itself, gathering evidence on the starting letter, number of syllables, etc., while another participant might work on what other factual information is related to the answer. During an insight problem, two participants might take radically different pathways to reach the same solution. These differences in approach affect the cognitive tools necessary to complete the task (i.e. semantic vs. episodic memory), and therefore might have different neural signatures, creating confusion or incorrect categorization of brain imaging results.

1.2 NEUROIMAGING AND NEUROPHYSIOLOGICAL RESEARCH

In fact, there are some differences in the neural activation maps for TOT and insight problem-solving. Through the use of fMRI, Maril et al. (2001) found greater activation during the TOT state in the anterior cingulate, right middle frontal gyrus, and right inferior frontal

cortex. Activity was greater in these areas than during both an immediate recollection of the item and an extended period of thought that ended in non-recollection without a TOT state. The authors suggest that the anterior cingulate functions as a retrieval monitor that becomes active when there is response conflict (i.e. the knowledge that the answer is right there, but the inability to state it). On the other hand, the right middle and inferior cortices are suggested to be representative of the potential retrieval approach. Right middle frontal gyrus has previously been implicated in the use of visuo-spatial tactics to working memory tasks, like mentally scanning a book to find the author's name (Awh, E. & Jonides, J., 1998).

In contrast, Jung-Beeman et al. (2004) found a different set of activations for an insight task. A compound remote associates task was used, in which three words are given that can each be made into a second word when combined with the same root word (i.e. pine, crab, and sauce turn into pineapple, crab apple, and applesauce, so "apple" is the target). In this task, situations of insight caused greater activation in the anterior superior temporal gyrus in the right hemisphere. The authors suggest that this activation is in accordance with the use of the area in language comprehension, particularly relating to novel or unusual semantic relations. Again, this seems to point to the relation of the activity to the type of cognitive approach used for the task. Importantly, unlike the behavioral TOT and insight results discussed above, the TOT and insight tasks described here actually access the same system (i.e. semantic memory). However, despite accessing the same system, the two tasks still activate different areas of cortex.

Extended periods of evidence accumulation have also been studied through the use of perceptual decisions made by macaque monkeys. Shadlen & Newsome (2001) recorded from single neurons in the lateral intraparietal sulcus (LIP) during a motion discrimination task in which a monkey discerned whether a series of dots on the screen were moving towards one

direction or another. The task started with fixation on the center of the screen, perception of the dots, and return to fixation of a center cue; upon extinction of the center cue, an eye movement indicated the motion direction. The direction of motion either moved towards the neuron's receptive field (RF), which caused an increase in firing, or away from the receptive field, which caused a decrease in firing. The authors also manipulated the coherence of the motion by changing the ratio of dots moving in one direction versus dots moving randomly about the screen. When more dots move together in one direction, the motion is more apparent. This should lead to a faster decision, because the evidence is readily available. On the other hand, less coherent motion might need to be studied longer to gather enough evidence towards the direction decision.

Importantly, Shadlen & Newsome (2001) found not only behavioral data that supported this hypothesis, but also coinciding neurophysiological data. The higher coherence of motion towards the RF, the faster the increase in firing in LIP. While lower coherence levels still caused increases in firing, the increase was slower and extended over a longer period of time. Conversely, higher coherent motion away from the RF caused fast decreases in firing, while lower coherent motion away from the RF caused slow decreases in firing. This suggests that the rate of neural firing is correlated with the amount of information or evidence available for the motion decision. When less information is available because fewer dots are moving together, it takes longer for the neural firing to reach a threshold for the decision.

Similarly, areas of primary and secondary somatosensory cortex were found to modulate firing rate according to the impending discrimination of either the roughness (Pruett et al., 2001) or vibration frequency (Hernandez et al., 2000; Salinas et al., 2000) of tactile stimuli. Pruett et al. (2001) swiped plastic squares with groove patterns across the fingertip of a restrained monkey.

They found that the average firing rate of neurons in the secondary somatosensory cortex predicted whether the monkey would classify the stimulus as smooth or rough. The correlation held true even when the force and speed of the stimulation was altered, and in fact lead to consistent errors based certain combination of groove pattern, force, and speed. Several researchers (Hernandez et al, 2000; Salinas et al., 2000; Romo & Salinas, 2003) conducted a similar experiment during which one grooved stimulus was vibrated against the fingertip of a monkey with varying frequency between trials. However, in this task the monkey was presented with two frequencies of vibration in sequence and had to indicate whether the second stimulus was faster or slower than the first. The average firing rate of neurons in the primary somatosensory cortex correlated with the monkey's discrimination.

Together, these neurophysiological studies suggest that extrasensory areas can modulate according to the coherence of a stimulus, and may be involved in mediating the decision to categorize the stimulus. However, there are several issues that arise from these studies upon closer examination. First, the areas involved in modulation according to the evidence are often closely tied to the type of stimulus present. For visual information, LIP is not a surprising candidate; a wealth of literature has described LIP involvement in visual perception and eye movements. The same can be said for primary and secondary somatosensory cortex and flutter/roughness discrimination; these cortices are the primary areas for touch information. These data together seem to suggest that there might be a separate evidence accumulator for each modality of stimulus. Is it possible to find a general evidence accumulator that functions across modalities? Second, the neurons found in these studies often fire for the sensory information, the accumulation of evidence, and the motor preparation before a decision. While this multi-tasking is certainly a parsimonious ideal for the brain, could this hold up for more complex decisions?

Third, the decisions used in the neurophysiological studies in monkeys are almost always explicit and dichotomous; the answer was either left or right, high flutter or low flutter. Although life might be simpler if each recognition or decision we made was dichotomous and explicit, this is not a realistic representation of the world. If someone waves to us from across a crowded conference hall, our options are not simply trying to recognize him as Bob or Fred. Instead, there are probably several acquaintances we might meet there, and we must peer through the crowd at the waving person to study the facial features to determine which acquaintance it is. Lastly, the use of monkeys inherently limits the types of tasks involved and the type of feedback we can collect. The tasks must be fairly simple in order to train the monkey quickly. While certainly slightly more complex tasks could be developed, it is highly unlikely that an open-ended memory search task like that of Maril et al (2001) or Jung-Beeman et al (2004) could work. We also cannot ask a monkey whether or not he feels he is close to making the discrimination, or if he has a sudden realization. This highlights the need to extend the research of evidence accumulation, and its neural substrates, to humans.

1.3 DIFFUSION MODELS

Some preliminary non-neurological human research has been the use of diffusion models to account for human behavioral data. Diffusion models describe the gradual tendency towards one bound or another, each potentially representing a decision or alternative. Once a threshold or bound has been reached, the decision it represents can be made. The rate at which evidence is accumulated toward one bound or another is called the drift rate. Often, these models include random walk, which allows the model to include some uncertainty and changes in accumulation

direction and drift rate, causing the trajectory towards the bounds to be more flexible, and account for the possibility of receiving both positive and negative bits of evidence. In psychology, diffusion models were first used to explain various forms of memory (Kinchla, R.A. & Smyzer, F., 1967; Ratcliff, R., 1978; Hockley, W.E. & Murdock, B.B., 1987; Ratcliff, R. & McKoon, G., 1988). Later, the use of diffusion modeling was introduced to sensory perception and discrimination. Ratcliff and Rouder (2000) fit data from a two-choice letter identification task and found that even though the visual item was quickly covered by a mask, the diffusion model that included a stable drift rate even beyond the masking point better predicted the data than a model that set the drift rate to zero upon masking. This model with the steady drift rate that continued beyond stimulus extinction also fit data from a brightness discrimination task (Ratcliff, 2002). This suggests that there is still a steady accumulation of evidence even once the stimulus has been masked or extinguished and there is no more visual information available. This would contrast with the ideal model of neuronal firing in the perceptual areas, which would stop once the visual stimulus is no longer present. While diffusion models are a nice illustration of the potential movement towards a decision in a mathematical form that nicely fits behavioral data, it is prudent to compare the models to actual neuronal phenomena.

Similar to the diffusion models used to account for human data as described above, several models have been developed to account for the macaque motion discrimination data. The general model suggests that the discrimination is made by comparing the activity in neuronal pools that code for motion towards or away from the response field (Shadlen & Newsome, 2001; Mazurek et al, 2003). Depending on the structure of the experiment, the decision is either made by selecting the option currently associated with more activity (if the decision is made under a specific time constraint) or waiting until one option reaches a threshold (if the decision is not

under a time constraint). However, it has been noted that whatever integrator is able to make the decision may also be influenced by knowledge of the outcome of previous trials, creating slight ongoing shifts in the likelihood ratio of one option over the other (Gold & Shadlen, 2001). This could potentially create a bias towards one decision, even before a stimulus is present. At lower thresholds, this may delay the correct response by nature of extending the amount of positive evidence needed to reach threshold, or could ultimately lead to an incorrect response by allowing the other option a head start in the diffusion. By including the comparison, integrator, and potential bias, diffusion models have accurately accounted for macaque data of motion and other sensory discriminations (Shadlen & Gold, 2004; Gold & Shadlen, 2001; Huk & Shadlen, 2005). Using a model similar to that which accounts for the macaque data, Palmer et al (2005) went on to mimic the motion discrimination experiment in humans and attempt to account for the human data. The diffusion model proved flexible enough to account for the standard experiment, plus variations that altered the speed instructions, response modality, and stimulus attributes, demonstrating the similarity of macaque and human responses in simple discrimination tasks.

1.4 CURRENT IMAGING LITERATURE

The use of diffusion modeling to account for the macaque data is promising, suggesting a connection between the neurophysiological data and the human behavioral diffusion models completed ~20 years prior. Palmer et al (2005) also showed that diffusion modeling continues to account for data even for motion discrimination in humans. However, motion discrimination is still a fairly simple task, and further highlights the need to expand studies of evidence

accumulation in humans using more complex decision-making tasks. On this track, several researchers have adopted simple perceptual recognition tasks for human participants. These tasks are often characterized by the masking or altering of visual stimuli to obscure immediate or obvious recognition, and then ask participants to categorize a stimulus into one of two categories. Heekeren et al. (2004) used grayscale pictures of faces and houses of which some were transformed with noise to obscure the image. Participants then categorized these images into either the "face" or "house" bins while in an fMRI scanner. The authors hypothesized that similar to the greater increase in firing for more coherent stimuli found in Shadlen & Newsome (2001), the easier to distinguish images should evoke greater activation in the areas responsible for the perceptual decision. This type of activation was found in left superior frontal sulcus, in the posterior portion of the dorsolateral prefrontal cortex. This area also modulated according to the difference in activation of the fusiform face area (FFA) and parahippocampal place area (PPA). This suggests that the left superior frontal sulcus is involved in the comparison computation between these two areas to make the categorization in this task.

Using a slightly different task, McKeeff, T.J. & Tong, F. (2007) also tested participants on a perceptual decision. Participants were shown Mooney faces, which are grayscale images remastered to only include black and white; this causes the obscuring of definite features, without losing the actual perception of a face. Control stimuli were made by taking the Mooney face stimuli and scrambling the image, so it includes the same patches of black and white, but without the perception of a face. Given the complexity of these stimuli, it took several seconds of viewing time for the participants to categorize each stimulus as either "face" or "nonface". The authors hypothesized that while activity in primary visual cortex should not change during the 12-second viewing window (since the visual stimulus is not changing),

activity might modulate in the FFA for items categorized as faces early versus late in the 12s window. This was in fact the case, as McKeeff & Tong found that activity in FFA modulated in time. That is, for items identified as faces early in the viewing window, activity in FFA rose more quickly than for those items identified later. In contrast, no modulation of this type was found in PPA; this was expected, since PPA is usually active during recognition of buildings and some objects.

However, Heekeren et al. (2004) and McKeeff & Tong (2007) have unfortunately incorporated one of the main problems already mentioned in reference to the neurophysiological studies. Despite having the capability to examine the whole brain through the use of fMRI, these human studies still focus on stimulus-relevant areas. So it is again not surprising to find modulation in these areas dependent on the amount of information available from the stimulus. In the case of McKeeff & Tong, the modulation of FFA most likely reflects the accumulation of visual information towards face recognition, but probably does not reflect a general perceptual decision area. Similarly, Heekeren et al. defined the area in left superior temporal sulcus by its modulation based on the comparison of activation in FFA and PPA. This suggests that this area might only be involved in perceptual decisions involving faces and houses, or perhaps visual objects in general. This highlights the need to find a task in which the perceptual activation itself can be distinguished from the cognitive processing involved in the recognition decision.

While these imaging studies have made headway on showing evidence accumulation in humans, these studies have mainly examined single timepoints; that is, the time at which the decision occurs. Though this can identify some of the regions involved in the decision and the potential accompanying experience of uncertainty, it ignores the dynamic nature of the decision-making process. Studies of the macaque monkeys have recorded from single

neurons over time (i.e. 2000 ms) during perceptual decisions; this has allowed for the examination of the timecourse of decisions. However, with the exception of patients undergoing certain neurological surgeries, there is currently an inability to gather single unit recordings from humans. This limits our ability to duplicate the macaque studies in humans on the single unit scale. Therefore, it was necessary to develop a perceptual recognition paradigm that extends recognition into a time envelope amenable to fMRI, a much more accessible option when studying humans.

2.0 METHODOLOGY

This section will first cover theoretical issues of the chosen methodology and the interaction of methodology and task, and then address the actual methods employed in the experiment.

2.1 LIMITATIONS OF FMRI

Considering the timecourse of activity leading to recognition, and how it differs dependent on the timing of recognition, gives insight into the potential mechanisms behind the process in humans. Development of an extended paradigm for fMRI allowed examination of not only the areas that are active at the recognition, but also the timecourse leading up to recognition, making comparison between the human and monkey data more plausible. Unfortunately, the use of fMRI is not without its limits. Magnetic resonance imaging capitalizes on the ability to align electrons in orbit around molecules by placing the subject in a strong magnetic field, and then "tipping" the electrons by a pulse of radio waves. The subsequent realignment of the electrons causes a warping of the magnetic field, which in turn alters the captured image. The warping of the image is then used to reconstruct the physical structure of the object. By changing the frequency of the radio wave, different contrasts can occur. Functional MRI relies on the blood oxygen level dependent (BOLD) contrast (Ogawa et al., 1990, 1992; Kwong et al, 1992), which uses a radio frequency pulse to disturb electrons on oxygenated hemoglobin in the blood. By

using techniques to vary the concentration of oxygen in the blood, Ogawa et al (1990) demonstrated that an increase in blood oxygen created a stronger contrast on the image. Conversely, techniques that decreased blood oxygenation were found to decrease the contrast.

Neural activity uses oxygen as an energy source, and therefore increased neural activity is associated with an increase in the removal and use of oxygen from hemoglobin in the blood. This causes an increase in the amount of deoxygenated hemoglobin in the blood. As mentioned above, a decrease in blood oxygen is related to a decrease in the BOLD contrast. This would then seem to posit that an increase in neural activity would cause a decrease in the BOLD contrast. Instead, an increase in neural activity also causes an increase in the local cerebral blood flow (CBF), allowing more oxygenated hemoglobin to arrive in the area of activity. Since the change in CBF outpaces the extraction of oxygen from the blood, it ultimately causes an increase in blood oxygen. However, the change in CBF takes several seconds to begin, allowing a momentary build up of deoxygenated hemoglobin. This temporary state has been considered the cause of the small dip in BOLD contrast prior to the rapid spike due to the increased oxygenated blood.

Further research has shown that changes in the BOLD contrast are consistent with changes in local field potentials, but not necessarily single- or multi-unit recordings (Logothetis et al., 2001). This suggests that a large amount of sustained neural activity is necessary to create an energy deficit that demands an increase in local blood flow for oxygen replenishment afterwards. It has been further suggested that the BOLD contrast may reflect the excitatory transmission of certain neurotransmitters, while failing to account for transmission by other (particularly inhibitory) neurotransmitters (Logothetis et al., 2001; Raichle, 2001; Attwell & Iadecola, 2002). Finally, as noted by Logothetis et al (2001), the connection between local field

potentials and BOLD activity raises an interesting question regarding the underlying signals that are represented in a BOLD image. Local field potentials have been shown to been related to neurons in the area receiving input and transmitting along local connections, rather than sending output to other areas. This suggests that the BOLD signal reflects the area that is receiving information, but may not reflect an area that is sending signal elsewhere.

The first limitation of fMRI for this study is the inherent evolution over time for the BOLD contrast. While ultimately the long evolution of the BOLD contrast will be useful for our data, there are some considerations that need to be addressed. First, the BOLD contrast demonstrates a ~1 - 2 second delay from the onset of neurological activity to the initial increase of oxygenated blood. This creates a potential problem of relating BOLD increases to specific transient and isolated events, such as a moment of insight versus the general longer evolution of decision-making. This will have to be considered in the data analysis. Second, the contrast can take up to 16 seconds to reach its peak for even a brief stimulus presentation. This means that if a task involves stimulation for several seconds, it is possible to lengthen the BOLD response simply due to stimulation, and not necessarily higher cognitive activity. A control or hypothesis must be developed for the comparison of purely sensory versus higher cognitive processing. Last, the BOLD contrast has a slow decrease down to baseline. This means that certain spacing of stimulus events may elicit an increase in the BOLD contrast prior to a return to baseline. However, several studies have proven that given proper inconsistent overlapping, this last consideration can be accounted for through the data analysis (Dale & Buckner, 1997; Friston et al, 1999).

The second limitation of fMRI is the ability to record information from the entire brain without knowing specifically what each area is doing at any given point in time. While the

ability to gather data on the entire brain initially seems like a blessing, it can instead create more confusion if specific hypotheses are not developed a priori for at least some of the areas. In this study in particular, the consideration of timecourses longer than the normal processing time of most cognitive functions (i.e. >8 seconds), compounds this problem by creating a plethora of complex multipoint data, some subsections of which might be doing similar things. Even with a priori hypotheses as to the potential timecourses of these subsections, the sheer amount of data is overwhelming. In order to initially tackle this problem, hierarchical cluster analysis will be used to organize the data into more manageable subsets. This technique will be discussed in more detail later on in the document.

The last major limitation of fMRI for this study is the amount of time necessary to create one whole image of the brain (repetition time; TR). The length of each whole brain image changes based on the strength of the magnet (and thus time needed to shift the magnetic field into alternate planes), the length and type of the radio frequency pulse, and the field of view. While TRs can range from 500ms-3000ms, the TR available for this study was 2000ms. This means that every 2 seconds a whole brain image was captured, and one data point was added to the timecourse. If we expect to compare the evolution of the BOLD response over time, a paradigm must be created that includes a decision that takes several seconds to develop and has enough variability such that timecourses of different lengths can be compared for changes in slope or rate of accumulation.

2.2 THE CURRENT PROJECT

To summarize the considerations outlined throughout this introduction, a task must be created that 1.) is simple, involving a fairly unambiguous approach, 2.) can separate perceptual processing from cognitive processing, and 3.) for the purposes of fMRI, can be extended in time.

Under these constraints, a picture recognition task was constructed for the current study. The task presented grayscale images that were revealed over the course of 16 seconds. In 2-second intervals, a black mask was slowly removed in random pieces. Participants were asked to respond when they could identify the picture, even if it was still partially covered by the black mask. This created a situation in which participants guessed pictures quickly (i.e. only 5% of the mask had been removed) or slowly (i.e. they waited until 25% of the mask was removed). This allowed for the comparison of faster versus slower evidence accumulation towards recognition. Using this task, several hypotheses are made:

1. Due to more of the picture being revealed over time, more visual information was present on the screen over time. Activity in perceptual areas should increase gradually over time in correlation with the change in visual information. However, since the revelation is consistent across all items in this task and does not directly impact recognition, this gradual perceptual accumulation should not modulate according to the time of recognition.
2. Given the subjective experience of gradual accumulation of evidence in tasks that evoke a TOT state (Maril, et al., 2001), combined with the modulation of activity found in both the neurophysiological and fMRI data, some areas should modulate in the rise of activity according to when the participants make a recognition decision. That is, for faster

identification, the slope of the BOLD signal should increase more sharply than for a slower identification. This is similar to the change in slope found in neural populations in LIP

(Shadlen & Newsome, 2001).

3. However, given the subjective experience of insight (Metcalfe, 1986, 1987), other areas might become active only at the point of recognition.

Lastly, due to the nature of the response instructions, motor planning and execution areas will be active at both the recognition and verification stages. This will allow for the separation of motor processing from decision-making during data analysis.The table below is included so that there is an item in the sample List of Tables.

2.3 EXPERIMENTAL METHODS

Two experiments were conducted on two separate groups of participants. Experiments 1 (Exp1) and 2 (Exp2) were nearly identical, except that we used within-trial jitter in Exp1 and added trials in Exp2. Experiment 1 was designed to identify regions of interest (ROIs) that contribute to perceptual recognition. Experiment 2 was designed to evaluate the timecourse of T_R-dependent activity in those regions. We chose this two-experiment approach for several reasons. First, comparing T_R and VoA events in Exp1 reduced the probability that ROIs would be related to motor processing. Second, because ROIs were defined using data from one set of subjects (Exp1) and applied to data from a different set of subjects (Exp2), the ROI-based timecourse data from Exp2 were not biased to show specific effects. Third, whereas within-trial jitter was needed in Exp1 to separate BOLD responses associated with recognition and VoA events, in Exp2 we

eliminated the within-trial jitter to reduce the complexity of the timecourses. In all cases below, anatomical labels and Brodmann's areas (BA) are approximate.

2.3.1 Participants

Participants were 31 right-handed, native English speakers with normal or corrected-to-normal vision (18 female, age 19-29 years). Four participants were excluded from analysis due to excessive movement and two were excluded due to data loss. Of the remaining 25 participants, 12 were run in Exp1 and 13 in Exp2. Some runs from four of the participants were excluded due to excessive movement. Informed consent was obtained in a manner approved by the Institutional Review Board of the University of Pittsburgh and participants received $75.

2.3.2 Stimuli

The pictures were 233 grayscale images (Rossion and Pourtois, 2004) reformatted into a standard 284 x 284 pixel image with a white background. Five images were reserved for the practice session; five lists of 12 (Exp 1) or 20 (Exp 2) pictures were randomly selected out of the remaining 228 pictures for task presentation. Each subject received his or her own randomly selected list set, ensuring that no participant received exactly the same set and order of images as another. The displayed images subtended an average 10.3° of the visual field and were presented against a black background.

2.3.3 Behavioral Paradigm

Testing consisted of five runs of a perceptual recognition task using picture stimuli, with 12 and 20 trials per run in Exp1 and Exp2, respectively. Runs were randomly intermixed with five runs from a related task, using word stimuli, which is not included in the current report. In each trial, stimulus revelation occurred over 8 discrete steps, each corresponding with acquisition of a whole-brain image (Fig 1a). In Exp1, the steps of revelation were randomly intermixed with six 2 s jitter periods, resulting in an average step duration of 3.5 s. Subjectively, jitter produced a pause of 2, 4, or 6 s between steps of revelation. In Exp2, the revelation steps occurred every 2 s without within-trial jitter. Between-trial jitter of 2, 4, or 6 sec (mean ITI = 4 sec) was included in both experiments to allow event-related analysis of individual trials.

At trial onset, pictures were covered by a black mask. The mask partially dissolved at each successive 2 s interval (i.e., revelation step) until pictures were completely revealed (see Fig. 1a). Participants were instructed to press a button when they could identify the picture with a reasonable degree of confidence (T_R). Neither speed nor accuracy were emphasized in the T_R response, and participants were not specifically encouraged to respond prior to full revelation. When stimuli were fully revealed, participants pressed the same button again only if their earlier recognition had been correct (VoA). We used gradual stimulus revelation over other unmasking procedures (e.g., mask degradation remains constant but areas revealed change from step to step) because we could readily map the quantity of stimulus input onto neural activity as a linear increase across the trial (e.g., Carlson et al., 2006). To help factor out basic lateralized motor signals in group analyses, response hand was counterbalanced across participants (Thielscher and Pessoa, 2007). Psyscope X was used for stimulus presentation and data collection (Cohen et al., 1993) (http://psy.ck.sissa.it).

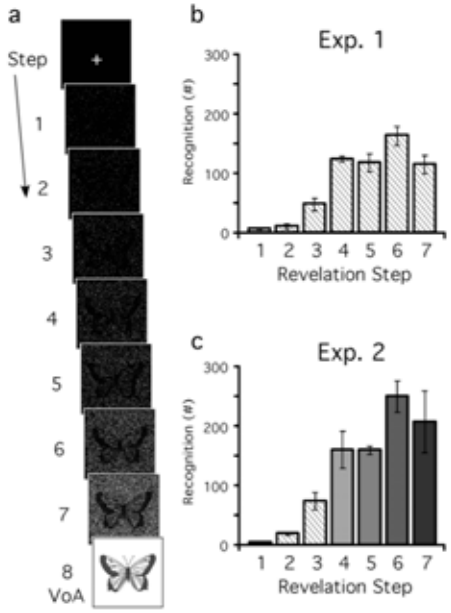

Figure 1. Task design and behavioral results.

a) The schematic illustrates the task design. In Exp2, revelation proceeded every 2 s until the object was revealed at the 8th and final step (14 s). In Exp1 (not depicted), jitter occurred during revelation. Subjects pressed a button when they could identify the picture with a reasonable degree of confidence, and again at VoA if earlier recognition had been correct. ITIs (jitter) varied from 2-6 s. Revelation steps are numbered (1-8). b-c) Distribution of T_Rs for Experiments 1 and 2, in 2 s bins. The total number of responses (s.d. bars) are plotted as a function of the step of revelation. In Exp1, recognition responses were collapsed to identify ROIs. In Exp2, bins were analyzed separately to identify time-dependent differences in BOLD fMRI activity. c) The levels of shading represent the four main conditions of interest in Exp2 imaging analyses.

2.3.4 Image Acquisition

Images were obtained using a Siemens Allegra 3T scanner. Visual stimuli were generated on an Apple iBook G4 with PsyScope X and projected onto a screen positioned at the head of the magnet bore using a Sharp PG-M20X digital multimedia projector via a mirror attached to the

head coil. Earplugs dampened scanner noise. Responses were made using a fiber optic button stick connected to the computer via an interface unit (Current Designs, Inc; Philadelphia, PA).

Anatomic images were collected using an MP-RAGE sequence (repetition time [TR] = 1540 ms, echo time [TE] = 3.04 ms, flip angle = 8°, TI = 800 ms, delay time [TD] = 0 ms). A series of whole-brain spin-echo echo-planar T2*-weighted functional images sensitive to the blood-oxygen-level-dependent (BOLD) contrast (TR = 2000ms, TE = 30ms, flip angle = 79˚, 2.2 x 2.2 in-plane resolution) were collected during testing. The first three image acquisitions were discarded to allow net magnetization to reach steady state.

2.4 DATA ANALYSIS

2.4.1 General Analysis

Imaging data from each subject were pre-processed to remove noise and artifacts, including: a) correction for movement within and across runs using a rigid-body rotation and translation algorithm (Snyder, 1996), b) whole brain normalization to a common mode of 1000 to allow for comparisons across subjects (Ojemann et al., 1997), and c) temporal re-alignment (using sinc interpolation) of all slices to the temporal midpoint of the first slice, accounting for differences in the acquisition time of each individual slice. Functional data were then re-sampled into 2mm isotropic voxels and transformed into stereotaxic atlas space (Talairach and Tournoux, 1988). Atlas registration involved aligning each subject's T1-weighted image to a custom atlas-transformed (Lancaster et al., 1995) target T1-weighted template using a series of affine transforms (Michelon et al., 2003; Fox et al., 2005).

Pre-processed data were analyzed at the voxel level using a general linear model (GLM) approach (Friston et al., 1994; Miezin et al., 2000). Details of this procedure are described by Ollinger and colleagues (Ollinger et al., 2001). Briefly, the model treats the data at each timepoint (in each voxel) as the sum of all effects present at that timepoint (*i*). Effects can be produced by events in the model (b) and by error (e). Thus, the equation for a given timepoint *i* is $y_i = a_{i,0}b_0 + a_{i,1}b_1 + \ldots + a_{i,M-1}b_{M-1} + e_i$, where $a_{i,m}$ is a coefficient relating the effect to the data at time *i* and M is the number of modeled effects. In matrix form this becomes $Y = \mathbf{Ab} + \mathbf{e}$, where **A** is the design matrix relating event types with time, **b** is a vector of events being modeled, and **e** is a vector of noise. Estimates of the timecourse of effects were derived from the model for each response category by coding timepoints as a basis set of delta functions immediately following onset of the coded event (Ollinger et al., 2001) (note that the number of timepoints in Exp1 and Exp2 was 9 and 16, respectively). Over each run, a trend term accounted for linear changes in signal, and a constant term modeled the baseline signal. Event-related effects are described in terms of percent signal change, defined as signal magnitude divided by a constant term. This approach makes no assumptions about the shape of the BOLD response, but does assume that all events included in a category (e.g., accurate T_R7) are associated with the same BOLD response (Ollinger et al., 2001). Thus, we could extract timecourses without placing constraints on their shape. Image processing and analyses were carried out using in-house software written in IDL (Research Systems, Inc.).

Group z-statistical maps were derived from the GLM using voxelwise repeated measures ANOVA with time as a repeated factor (Winer et al., 1991). The ANOVA implementation produces a set of main effect and interactions images determined by the factors in the design (Schlaggar et al., 2002). The main effect of time image identifies voxels in which

the temporal profile over the analyzed time period is not flat (i.e., no change in signal). Interaction by time images identify voxels in which activity differs across levels of factors as a function of time. Following is a description of data analysis procedures specific to each experiment.

2.4.2 Experiment 1: Region selection

The goal of this analysis was to define regions that showed differential activity at the time of recognition (T_R), independently of when it occurred in the trial, with activity elicited at the time of verification (VoA). A subset of these regions could be specifically related to the time of recognition. Events were coded into the voxel level GLM as follows. Recognition responses occurring before VoA were collapsed into a single T_R condition. Trials with single responses occurring at the VoA stage ('end-trial recognition') were coded separately in the GLM, but were not included in statistical analyses reported here. Trials were sorted by self-reported accuracy (earlier recognition response correct, incorrect) and coded separately according to accuracy. Note that a VoA response only occurred on trials that were scored as correct. Trial events were modeled over nine timepoints (18 s) beginning at the time of response. Overall, 6 regressors were coded in each participant's GLM: T_R, VoA correct, VoA incorrect, end-trial recognition, trend, and baseline.

We wanted to identify regions associated with the recognition decision, while at the same time minimizing the extent to which the observed accumulation effects were related to action planning and initiation. To this end, we identified voxels in which activity differed at T_R and VoA by entering the T_R and VoA events into a repeated measures ANOVA (Winer et al., 1991) with event-type (T_R, VoA) and time (9 timepoints) as factors. This analysis produced a

number of main effect and interaction images. The interaction of event-type and time image identified voxels in which activity related to T_R and VoA differed over time. We used this image to derive regions of interest that were 1) likely to be involved in the recognition process and 2) unlikely to be directly related to motor planning or execution. Note that we also counterbalanced response hand across subjects to factor out the signals arising from lateralized motor processing areas (Thielscher and Pessoa, 2007). Functional ROI volumes were defined by growing regions around peak voxels using algorithms developed by Abraham Snyder (Wheeler et al., 2006). This procedure resulted in 73 ROIs (Tables 1-4).

2.4.3 Experiment 2: Timecourse analysis

In Exp2, we removed within-trial jitter from the revelation paradigm in order to evaluate the evolution of the BOLD response over a period of regularly increasing stimulus information. The aim was to find differential timing of activity related to different times of recognition.

Events were coded into each participant's GLM as follows. Recognition responses were binned into seven categories according to the step of revelation (T_R1-7) in which they occurred. These categories were further subdivided according to recognition accuracy as denoted by the verification response (correct, incorrect). Trials with single responses occurring in the VoA stage ('end-trial recognition') were not further categorized and were coded separately in the GLM. As in Exp1, trend and baseline terms were also modeled, resulting in 17 possible regressors (T_R1-7 correct, T_R1-7 incorrect, end-trial recognition, trend, constant) for each subject. While trials were 16 s in length, each event was modeled over 32 s (16 timepoints) to account for the lagged hemodynamic response.

Using ROIs defined in Exp1, we next extracted timecourses for a subset of Exp2

conditions. Behavioral data indicated that most correct recognition responses occurred in steps T_R4-7 (Fig. 1c, shaded bars). To maximize power, imaging analysis focused on correct T_R4-7 trials. Recognition decisions that were judged to be incorrect were also analyzed, but the data are not included in this report. The primary focus is on evaluating the influence of the timing of T_R on the shape of the hemodynamic response, including timing of onset, peak, and width waveform components.

2.4.4 Initial definition of dataset using hierarchical cluster analysis

The development of an extended decision-making task for use in fMRI requires the consideration of the large amount of data that will result. For each trial, data points for each region will be gathered for every 2-second timepoint over the course of 16 seconds. Due to the extended shape of the BOLD response, the actual window of time for the analysis will be extended to 30 seconds. This means that the total dataset will include 30 data points for over 200 trials in each of the 70+ regions. Even with averaging by grouping trials into 2-second response bins, the dataset will still include 30 data points for 4 conditions in each of the 70+ regions. In the end, this will create a dense dataset that will need to be organized for ease of analysis. Taking a cue from genetic analysis, one fast and easy way to organize data is to use cluster analysis. Through the use of cluster analysis, data can be organized into clusters with similar value profiles. Classification of similarity can be considered through compactness, connectedness, or spatial separation (Handl et al, 2005). While connectedness would be an easy way to cluster the data according to location within the brain, the goal of the current study is to find brain areas with similar temporal profiles regardless of location. To this end it is most useful to use a cluster

analysis based on compactness, which will allow clustering of non-neighboring items with low variation in temporal data profile. That is, each area within a cluster should have a similar BOLD response across the trial, even if located far away from all other areas in the cluster. The specific cluster technique used for the current data is a hierarchical cluster analysis using the un-weighted paired group method with arithmetic mean (UPGMA).

For the current picture data, the following steps were taken to complete the cluster analysis:

1. Divide the data in bins according to time of response. The first three bins were removed from further analysis due to insufficient numbers of trials.
2. For the remaining four response bins, the timecourses were extracted from the regions defined by the first experiment.
3. For each region, the four timecourses were stacked end-on-end to create one “super timecourse” for the region.
4. Every “super timecourse” was then correlated with all the other “super timecourses”. This develops the resemblance matrix filled with the correlation coefficients for each pair comparison.
5. Once the matrix is complete, clustering via UPGMA can occur. This method involves finding the most similar pair in the matrix and combining them into one entity (a cluster). This also deletes the individual correlation values of the two regions with all other regions, and replaces it with a correlation value for the cluster compared to all other individual regions.
6. With the adjusted matrix, the most similar pair is again found and combined into a cluster. This causes a new deletion and replacement of correlation values to remove the individual correlations and replace them with correlations involving the new cluster.

7. This step is repeated until there are no more merges possible (i.e. everything is clustered together).

After finishing the cluster algorithm on the matrix, the clusters can then be represented in dendrogram format. In this format, regions are connected to their most similar neighbor(s) by a direct branch, while slightly less similar neighbors are connected through longer branches, and the longest branches connect even less similar neighbors. Where the cross-brace of a branch occurs on the scale on the dendrogram indicates the distance coefficient of the cluster. The distance coefficient is equal to 1-r, or the amount of variability not accounted for within the cluster; the smaller the distance coefficient, the more similar the regions.

One thing to note is that UPGMA, while perhaps the most popular cluster algorithm due to simplicity and availability in statistics packages (Handl et al, 2005; Romesburg, 1984), is not the only option for cluster analysis. One potential alternative is single-linkage, which is similar to UPGMA with one exception. While clusters are still formed from the most similar pair in the current matrix, the adjustment of the matrix after creating the cluster is slightly different. Instead of reformulating the correlations to reflect the correlation with the newly combined cluster as a whole, single-linkage simply takes the smaller distance measure (or higher correlation) of the regions combined into the cluster. For example, consider if region A has a distance coefficient of 10 with region C, and region B has a distance coefficient of 12 with region C. If regions A and B are combined into a cluster, different values for the correlation with region C would result depending on the cluster algorithm. Under UPGMA, cluster AB would have a distance coefficient of 11 with region C. However, using single-linkage, cluster AB would have a distance coefficient of 10 with region C, because this is the smaller distance coefficient from the two combined regions (Everitt, 1993). While the two approaches are

extremely similar, UPGMA was selected for this analysis due to the more accurate distance coefficients that account for the relationship between groups of areas, rather than the "staircase" results found using single-linkage.

2.4.5 Secondary analysis with linear interpolation

The linear interpolation assumes that a straight line connects each pair of data points in succession, and assigns 1000 data points to this line. This turns each timecourse into a string of 15,000 data points. From this string, several specific data points are identified as key features as follows:

1. Peak – the point at which the highest value occurred
2. Onset – the point at which activation exceeded ~15% of the peak activation value
3. Full-width, half-maximum (FWHM) – the distance between the two points, centered around the peak point, at which activation is 50% of the peak activation value

It should be noted that the threshold for the onset point is somewhat arbitrary. To account for possible differences, values were extracted at 10%, 15%, 20%, and 25% of the peak activation. Since there was no difference among these values, the average was taken and used at the onset value. Once these values were extracted for each of the four conditions for each of the regions, the values were collapsed into a 1x12 vector of values (3 values for each of the 4 conditions). These new strings of values were then clustered using UPGMA to separate the positive timecourses into more specific categories.

3.0 RESULTS

3.1 BEHAVIORAL ANALYSIS

3.1.1 Experiment 1

In the group analysis (n = 12), 620 of 704 picture trials received a recognition response during steps 1-7 (T_R1-7) of revelation. Of these, 564 (91.0%) received a VoA response and were thus judged to be accurate. The 84 recognition responses occurring in step 8 (VoA) were not scored because the pictures were by then fully revealed, and recognition and VoA occurred simultaneously. The distribution of responses was examined by binning recognition times (RTs) on correct trials at 2 s intervals, time-locked to the acquisition of a whole-brain fMRI volume. Binning produced 7 categories of response, each associated with a step of revelation (T_R1-7). As shown in Figure 1b, most correct responses occurred in T_R4-7.

3.1.2 Experiment 2

In Exp2 (n = 13), 985 of 1148 trials received a recognition response prior to VoA. Of these, 852 (86.5%) received a later VoA response. The distribution of binned correct trials was quite similar to the distribution from Exp1 (Fig. 1c), with 157, 156, 247, and 204 in T_R4-7, respectively. Data from the two studies demonstrate that gradual revelation produced significant

spread in recognition times.

3.2 IMAGING RESULTS

3.2.1 Experiment 1

To identify regions involved in perceptual recognition, but not motor execution, T_R and VoA events were compared using a repeated measures ANOVA (see Methods). This analysis revealed significant differences ($p < .0001$, uncorrected) between recognition and VoA activity in many regions including bilateral calcarine sulcus, cuneus (posterior occipital), precuneus, inferior temporal cortex (IT), posterior parietal lobes (PPL), anterior insula near the frontal operculum (aI/fO), striatum, dorsal anterior cingulate cortex (dACC), medial frontal gyrus near the pre-SMA (meFG/pre-SMA), and dorsolateral prefrontal cortex (see Tables 1-4). From this map, we derived regions of interest around peak voxels (10 mm radius, 10 mm consolidation distance between peaks) and masked out voxels that failed to pass multiple comparison and sphericity corrections (see Methods). This procedure produced 73 ROIs (Fig. 2, middle panel; Tables 1-4), which were then used in Exp2 to examine the evolution of T_R-dependent BOLD activity during non-jittered revelation.

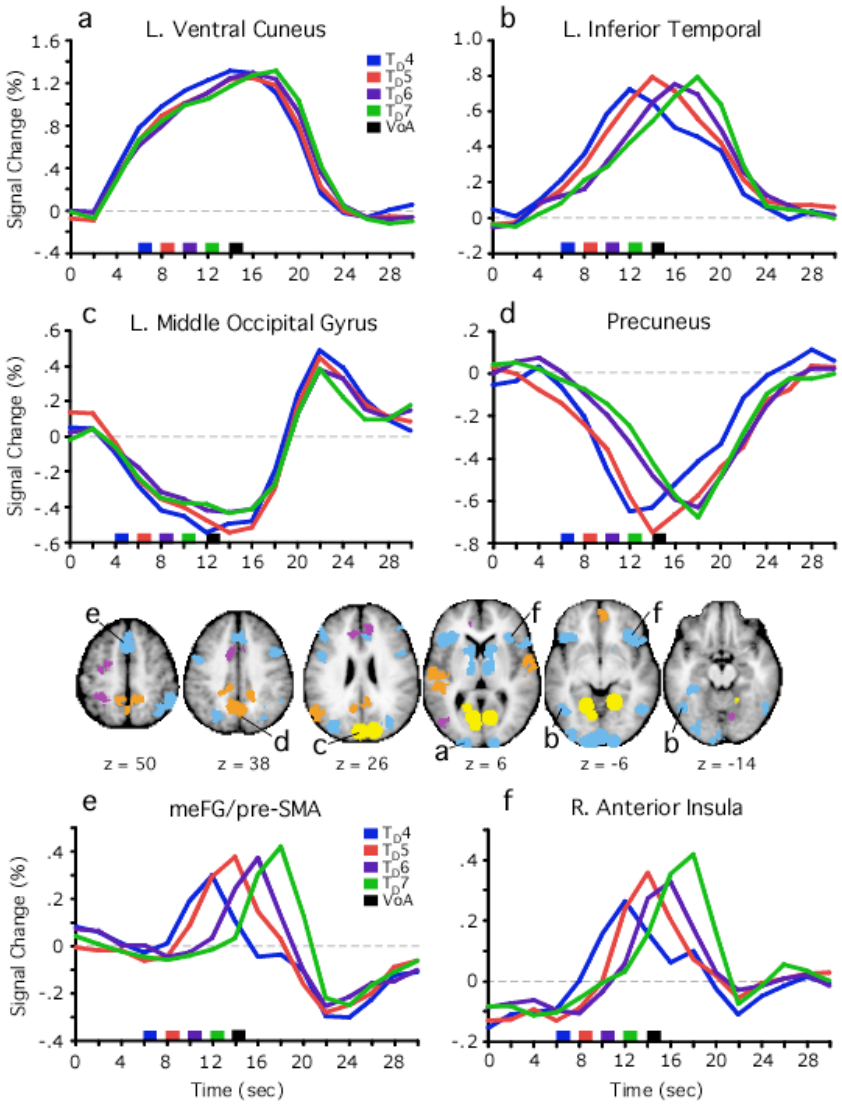

Figure 2. Select regions of interest and their timecourse data.

Regions of interest from Exp1 are shown near center, color-coded by Exp2 cluster membership at 1 - r = 0.8 (see Fig. 4). ROIs are displayed in horizontal slices over the top of the anatomical template used in stereotaxic atlas transformation. Difference in mm from AC-PC is noted below each slice. In a-f**, timecourses for T_R4-7 are graphed, in units of percent signal change from baseline (0%), as a function of time. Timecourses are color-coded according to the legend. T_R1 began at 0 s. The onsets of steps 4-7 are denoted by different bar colors on the x-axis, as denoted by the legend. Step 8 (VoA), which began at 14 s, is denoted by a black bar on the x-axis. Note that there is no timecourse for VoA.** a**) left ventral cuneus (peak voxel coordinate, -19, -99, +2),** b**) left IT (-42, -63, -9),** c**) left cuneus (-1, -83, +25),** d**) right precuneus (+2, -60, +37),** e**) meFG/pre-SMA (-1, +14, +51),** f**) right aI/fO (+33, +22, -2).**

3.2.2 Experiment 2

3.2.2.1 Predictions

Based on basic principles of linear systems, including scaling (output magnitude is proportional with input magnitude) and superposition (total response to multiple inputs equals the sum of the responses), we hypothesized that various cognitive events could influence the shape of the evolving BOLD signal. These events include sensory processing, evidence accumulation, recognition decisions, verification decisions and overt behavior. Because stimuli were revealed gradually from under a black mask, the amount of stimulus information increased at regular intervals throughout the trial. Accordingly, in visual processing areas which process basic stimulus features, the BOLD signal should begin to increase early in the trial and continue to increase as the stimulus is revealed. Thus, as shown in Fig. 3a, the width of the timecourse profile in sensory processing areas should correspond to trial duration (16 s). In contrast, the neurophysiological findings (Kim and Shadlen, 1999; Shadlen and Newsome, 2001) predict that activity in accumulation regions will begin early in the trial and continue to increase at a T_R-dependent rate. For instance, recognition at T_R4 should be associated with a more rapid increase in activity than recognition in T_R7 (Fig. 3b). Based on the findings reported in the literature we may find accumulating patterns of activity in parietal and frontal areas. Given the task demands, we may also find task-specific ROIs that are important in visual object processing. BOLD responses associated with processes engaged at the moment of recognition should also vary according to T_R. Because the moment of recognition is a discrete event, responses should occur transiently at T_R (Fig. 3c). A large body of literature on decision making (e.g., Bush et al., 2002; Carlson et al., 2006; Grinband et al., 2006; Hampton and O'Doherty, 2007; Thielscher and Pessoa, 2007) implicates anterior cingulate and frontal opercular regions in this type of

processing. Accordingly, we hypothesize that these regions will be recruited at the moment of recognition. Although the timecourse profile predictions are derived from theoretical accounts and empirical findings, we note that BOLD responses need not necessarily show these specific timecourse patterns because some regions may show combinations of such responses (i.e., both accumulator and moment of recognition patterns, which would preclude dissociation), or show responses not otherwise considered *a priori*.

According to these expectations, the pattern of activity associated with accumulation and the moment of recognition should have some similarity. For example, because accumulation and recognition are inherently associated with T_R, the time to peak activity (*peak*) for both should shift in time as a function of T_R. However, as illustrated in Fig. 3b - 3c, they should differ in two important ways. First, because of a role in integrating information over time, BOLD responses associated with accumulation should increase as soon as information related to a decision becomes available (e.g., earlier *onset*; Fig. 3b). In contrast, the onset of activity associated with the moment of recognition should shift later in time depending on T_R (Fig. 3c). Second, because evidence gathering is a prolonged process, timecourses associated with accumulation should be more extended in time (i.e., greater *width*), albeit showing narrower widths than regions related to visual processing. Combined, these two predictions further predict that in accumulation (but not moment of recognition) ROIs the slope of the leading edge of the BOLD response will decrease as T_R increases. It is important to emphasize that, despite the preceding hypotheses describing event-dependent time course shapes, we did not explicitly model the shape of the hemodynamic response.

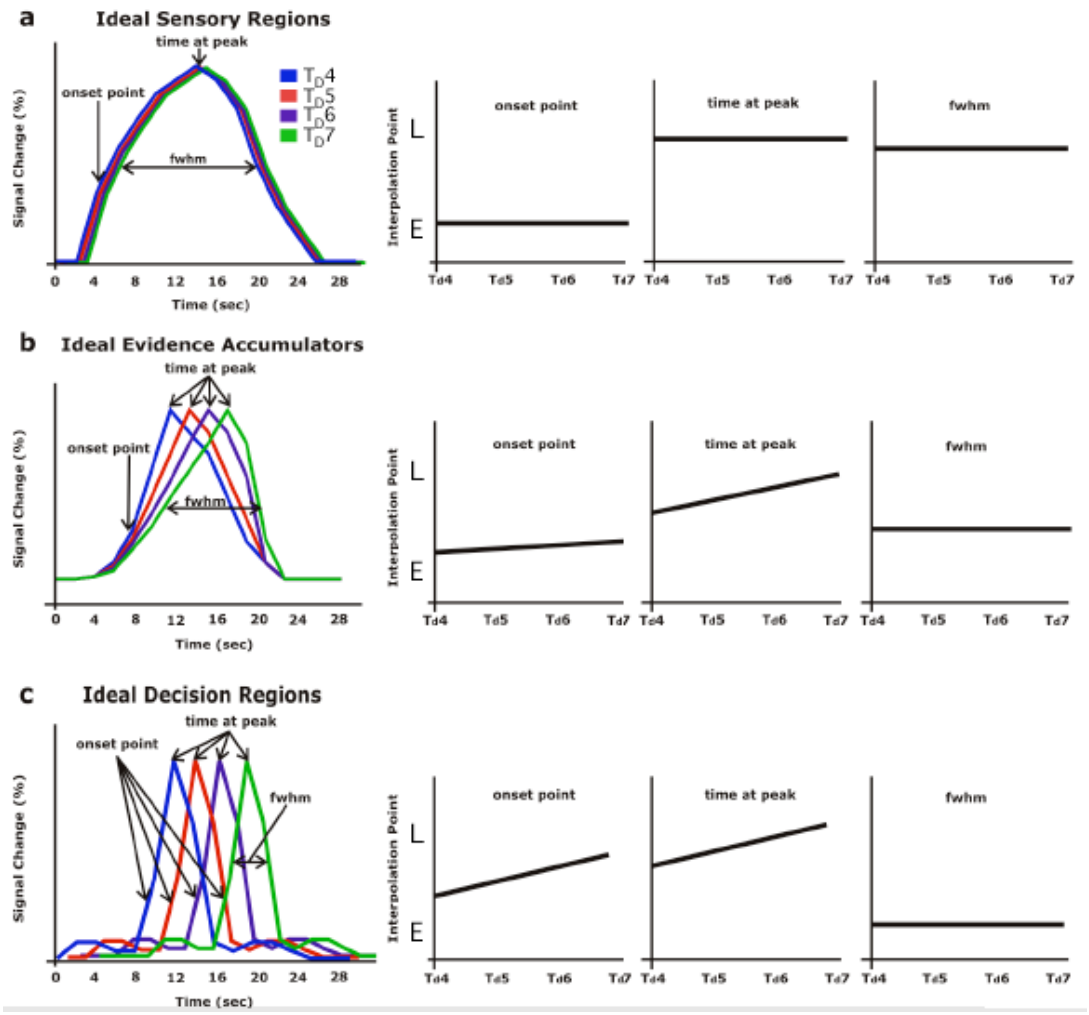

Figure 3. Idealized timecourse patterns in Exp2

related to a**) sensory processing,** b**) accumulation, and** c**) moment of recognition processing. The graphs to the left depict time-dependent signal change (arbitrary units) in perceptual recognition at four different, successive, T_Rs (T_R4-7).** a**) In sensory areas, none of timecourse onset, peak, or FWHM were expected to vary as a function of T_R, but responses should be extended in time.** b**) Because evidence gathering should begin when information becomes available, only time-to-peak in activity was expected to vary with T_R in accumulators.** c**) Both onset and peak times should vary in moment of recognition regions that become active at the time of recognition. This late, discrete response should produce a narrow timecourse.**

3.2.2.2 Hierarchical cluster analysis

From the 73 Exp1 ROIs, we extracted T_R-dependent timecourses from the Exp2 trials in which recognition occurred during revelation steps 4-7. We wanted to characterize the similarities and differences in patterns of timecourses across a large set of ROIs, so we began sorting the data using a hierarchical cluster analysis (See Methods). Fig. 4a displays the relationships among the 73 ROIs using a cluster tree (dendrogram). Regions with similar patterns of timecourse are clustered more closely than regions with different patterns. Pruning the cluster tree at 1 - r = 0.8 produced four clusters, each associated with a distinct pattern of timecourse when averaged over all ROIs in a cluster (Fig. 4b-e; Tables 1-4). A large cluster of regions located in medial parietal (precuneus) cortex, superior temporal gyrus, posterior insula, medial frontal cortex, and lateral parietal lobes exhibited negative timecourses that tended to peak in step with T_R (Fig. 4b; Table 1). A cluster of 7 ROIs located in bilateral posterior occipital cortex, lingual gyrus, and left parahippocampal gyrus displayed an initial decrease in activity, followed by a prominent increase near the end of the time series (late positive; Fig. 4c, Table 2). A third cluster included ROIs near left middle frontal gyrus (~BA 6), PPL, and middle temporal gyrus, and a subset of the ROIs found in bilateral ACC (BA 32, 24). These regions displayed a bimodal response, with an initial positive response that corresponded with T_R and a secondary positive response near the end of the time series (Fig. 3d, Table 3). The fourth and largest cluster displayed positive responses that, as a group, suggested increased activity at a rate corresponding with T_R (Fig. 4e Table 4). These ROIs were located in bilateral dlPFC (~BA 47, 46), ACC (BA 32), IT (including fusiform gyrus; BA 37, 20), PPL (BA 40, 7), cuneus/posterior occipital (BA 18), striatum, thalamus and cerebellum, and represent the target of our further analyses.

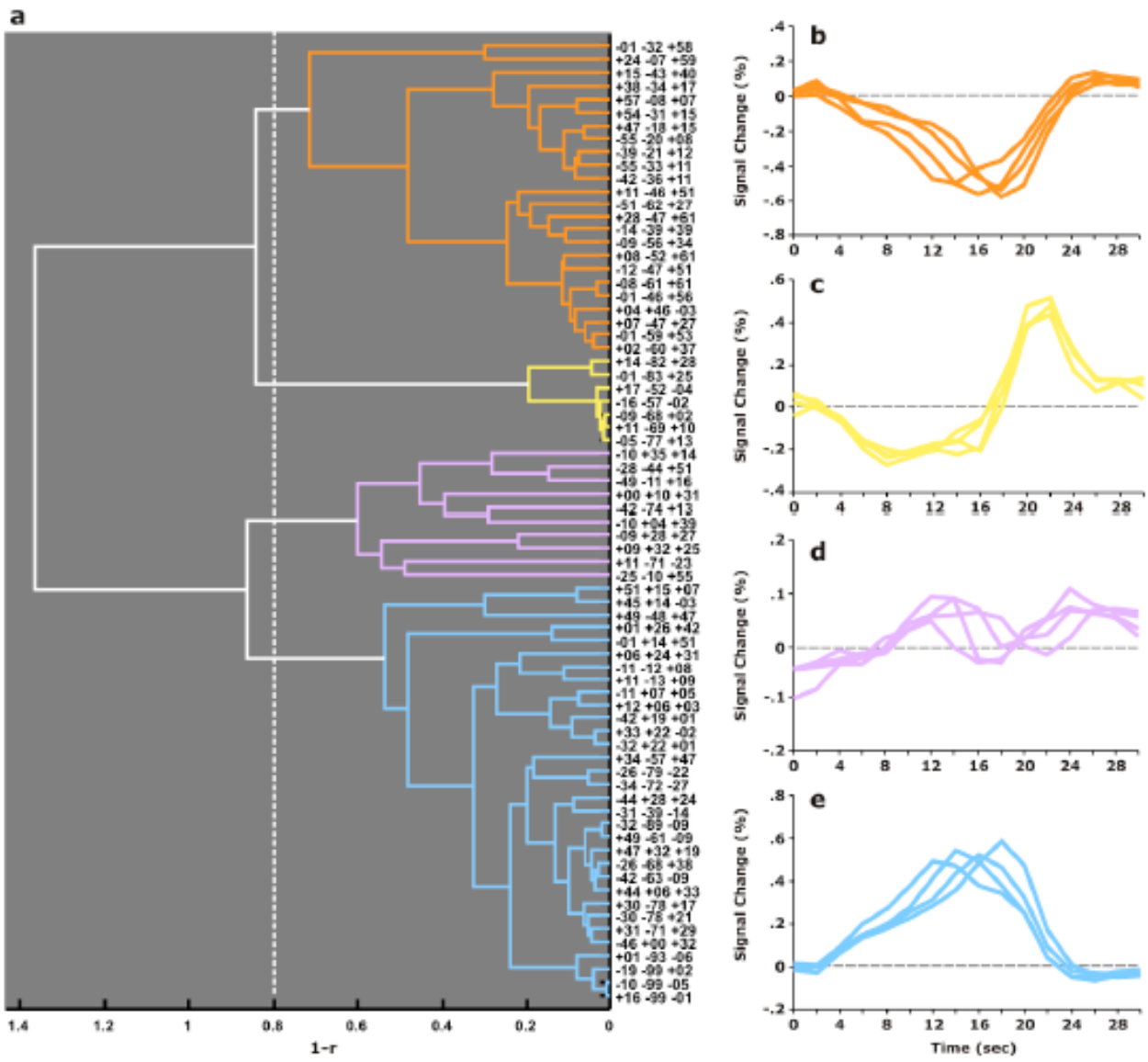

Figure 4. Cluster tree and averaged T_R-dependent timecourses.

a) **The cluster tree displays the similarity of timecourses across ROIs in terms of a distance unit (1 - r). ROIs linked across greater distances on the x-axis exhibited more disparate timecourses. As 1 - r values approach 0, timecourse similarity increases. As 1 - r increases above +1.00, timecourses become negatively correlated. The vertical dashed line shows where pruning the tree at 1 - r = 0.80 separated the tree into 4 major clusters. The cophenetic correlation coefficient was 0.8234, suggesting very little distortion in the data in order to construct the tree.** b-e) **Timecourses for T_R4-7 are averaged across all ROIs in each major subcluster, and across graphs the timecourses are color-coded by cluster membership and are graphed, in units of percent signal change from baseline (0%; horizontal dashed line), as a function of time.**

Fig. 2 shows representative timecourses from six ROIs: a) left ventral cuneus near BA 17 (Talairach atlas z = -19, y = -99, z = 2), b) left IT near BA 37 (-42, -63, -9), c) middle occipital gyrus near BA 18 (-1, -83, +25), d) precuneus near BA 7 (2, -60, 37), e) meFG/pre-SMA near BA 32 (-1, 14, 51), and f) right aI/fO (33, 22, -2). The plotted time series extend over 16 frames of image acquisition (32 s) and are shaded according to T_R. Even in individual ROIs, there were clear time course patterns evident in the large positive cluster (Table 4). For example, early visual processing areas displayed an early onset of BOLD signal change, followed by a gradual increase in activity that extended to the end of the trial (e.g., left ventral cuneus near BA 17, Fig. 2a). In these regions, activity corresponded mostly with the amount of visual information on the screen. This type of response is consistent with a 'sensory processor' (Fig. 3a) that processes basic sensory information but may not contribute directly to higher order recognition analysis. In other regions with an early onset, the peak in activity shifted with T_R. This set included ROIs in bilateral PPL, precuneus, middle occipital gyrus (MOG), left IT (Fig. 2b) and bilateral dlPFC (Table 4). This pattern of accumulation is consistent with the predicted behavior of an evidence accumulator (Fig. 3b) that integrates information over time. In contrast, BOLD responses in bilateral aI/fO (Fig. 2f), dorsal ACC, meFG/pre-SMA (Fig. 2e), and thalamus were markedly more transient, with onsets and peaks that appeared to correlate positively with T_R. Activity in these regions appeared to be most directly related to processes engaged at the time of recognition. The cluster analysis also identified two patterns of negative response. For example, ROIs near the lingual gyrus and cuneus (~BA 19; Fig. 2c) showed an initial decrease in activity followed by a marked increase near the end of the trial. In other regions near the angular gyrus and the precuneus (Fig. 2d), activity appeared to decrease at a rate corresponding with T_R. Due to space considerations, we will focus on the positive responses.

3.2.2.3 Linear interpolation of BOLD responses

We next investigated time course patterns from the positive-going cluster (Fig. 4e) by quantifying onset, peak, and full width at half maximum (FWHM) for each of the 32 ROIs. Our predictions across levels of T_R for sensory processors, accumulators, and moment of recognition ROIs are displayed in Figure 2. To objectively classify ROI behavior based on these attributes, we entered the onset, peak, and FWHM values into a second hierarchical cluster analysis. Thus, in contrast to the previous cluster analysis (Fig. 4) where we correlated the timecourses between ROIs, the goal of the second cluster analysis was to correlate interpolation parameters in the 32 positive ROIs. Interpolation data for each ROI took the form of a 1 x 12 vector representing the four onset points (T_R4-7), four peaks (T_R4-7) and four width values (T_R4-7). For reference, we also included the idealized values for each predicted response type displayed in Figure 3. The results of the second cluster analysis are displayed in Fig. 5, with idealized parameters labeled "accumulator", "sensory", and "recognition". The 32 ROIs clustered into three distinct groups containing 14, 5, and 13 ROIs (not including the three idealized value sets). Within each group, some ROIs clustered quite closely with the idealized parameters. For example, regions in medial occipital cortex (~BA 17/18) clustered closely with the idealized sensory processing parameters (Fig. 5a, red). Responses in occipital and fusiform ROIs clustered quite closely with the idealized accumulator parameters (Fig. 5a, blue). Regions in medial frontal gyrus (meFG) (~BA 6), ACC (~BA 8, 32), right inferior parietal cortex (~BA 40), right IFG (~BA 47) and right inferior precentral gyrus (~BA 44) clustered tightly with the idealized moment of recognition parameters (Fig 5a, green). A number of other ROIs, however, were associated with parameter differences that led to greater cluster distances. For example, ROIs in frontal and parietal cortex displayed response parameters similar to the idealized accumulator, but tended to have larger fwhm values

than ideal. Overall, however, the moment of recognition ROIs were clearly distinct from the accumulator and sensory processing ROIs.

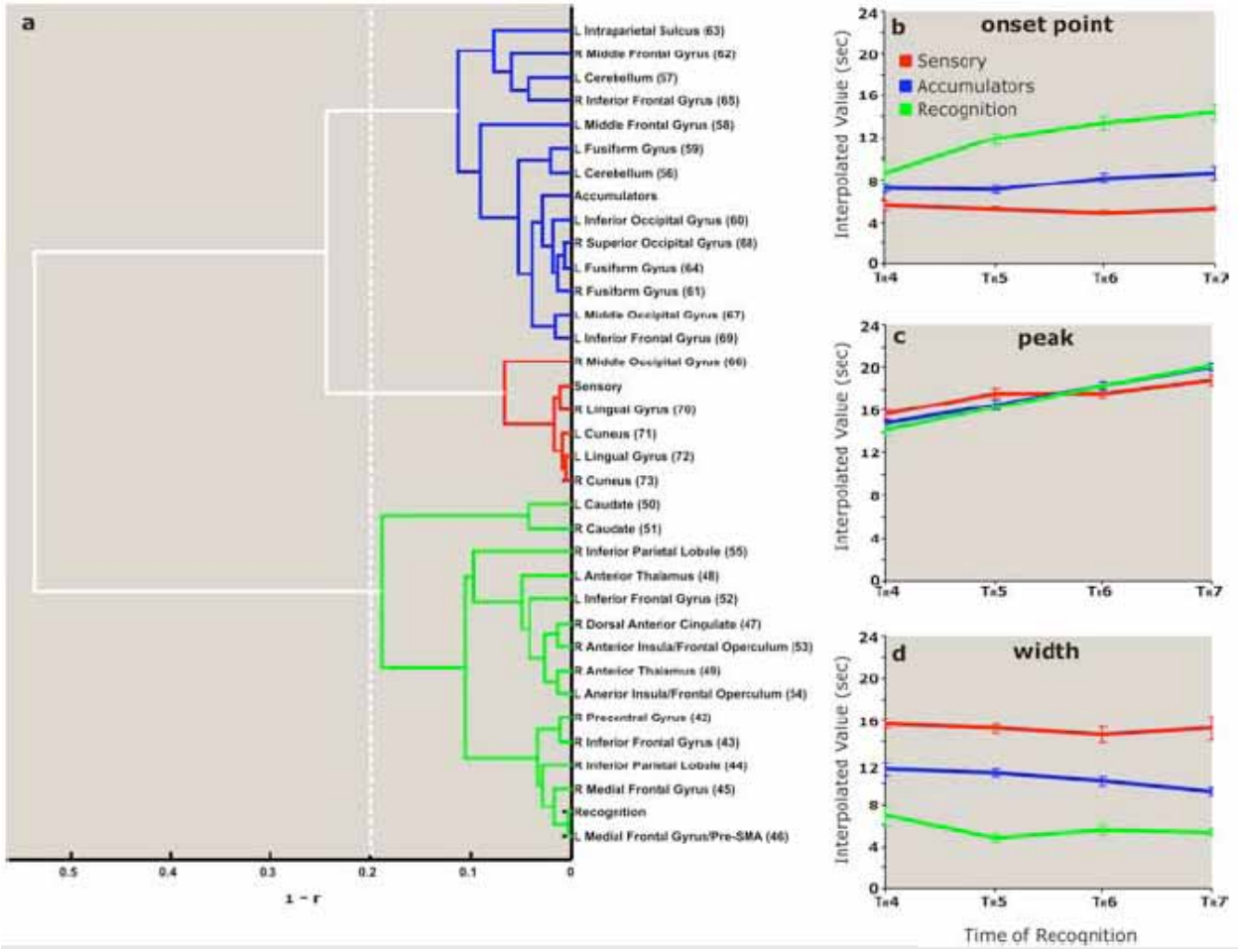

Figure 5. Hierarchical cluster analysis of interpolation data.

Each of the 32 ROIs from the positive waveform cluster were subjected to interpolation analysis that defined each region's onset point, peak, and width. a) **Cluster tree representing the three categories of regions based on the predicted outcomes from Figure 2. (Red = Sensory Processors; Blue = Accumulators; Green = Recognition Regions). The cluster was cut at a 1-r value of 0.2 to allow for each region to belong to a distinct cluster. The ideal values from Figure 2 were also placed into the correlation matrix in order to determine which of the 32 regions clustered near to or far from these hypothesized categories.** b-d) **Mean interpolation values for each of the three sets of regions identified in the cluster analysis separated by onset point, peak, and width. Bars represent standard error of the mean (SEM). Note that the slope of increasing peak times (5c) in sensory ROIs differed significantly from accumulation and recognition ROIs.**

We next averaged the timecourses at each T_R across all ROIs in each cluster group to investigate the patterns of response (Fig. 5b-d). At this broad level, the group patterns were consistent with our predicted responses for sensory processors (Fig. 5b), accumulators (Fig. 5c) and moment of recognition (Fig. 5d) processing. The cluster tree is color-coded according to the response type: blue for those consistent with the predicted accumulator response, red for sensory processor, and green for moment of recognition. To preserve space, we will refer to these clustered groups as "sensory", "accumulation", and "recognition" groups.

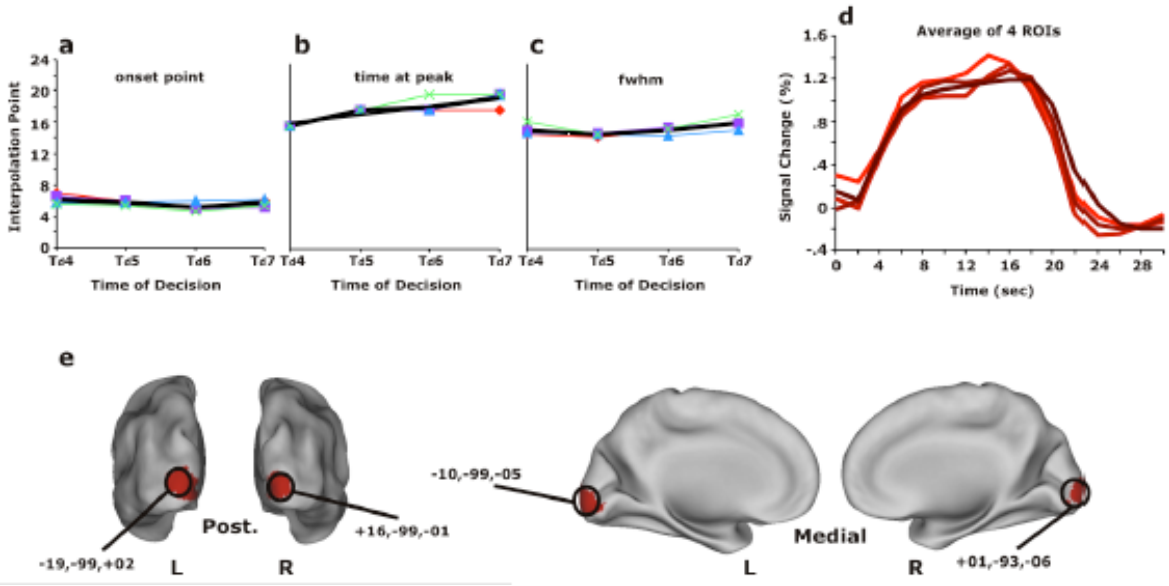

Figure 6. Interpolation analysis, sensory processors.

a**) time courses for five sensory ROIs identified by the interpolation analysis. Time courses are shaded by T_R (see Fig. 4 caption)** b-d**) The data for each sensory region is shown in red and the mean of those values is indicated by a thick black line for onset, peak, and width** e**) The ROIs are shown projected onto inflated cortical surfaces of left and right hemispheres. L = left; R = right; Post. = posterior; T_R = step in which recognition occurred.**

Figures 6, 7 and 8 (a-c) show the interpolation values plotted for each ROI in the three main categories, as well as the average values represented by a thicker black line. Onset times in

sensory ROIs (Fig. 6a) changed little across T_R4-7 (mean = 2.8, 2.6, 2.4, 2.6 sec, respectively, across ROIs within the cluster), while onset times in accumulator ROIs (Fig. 7a) increased slightly (3.5, 3.5, 4.1, 4.3 sec). In recognition ROIs, onset times (Fig. 8a) increased markedly as T_R increased (4.2, 6.0, 6.7, 7.1 sec). Peak times tended to increase in all three region types (Fig. 6-8b), with steeper increases in accumulator (7.4, 8.2, 9.2, 10.0 sec) and recognition (7.1, 8.2, 9.2, 10.1 sec) ROIs than sensory (7.8, 8.8, 8.8, 9.4 sec) ROIs. Sensory ROIs were associated with the widest response profiles across levels of T_R (Fig. 6c; 7.8, 7.6, 7.3, 7.6 sec), followed by accumulator (Fig. 7c; 5.7, 5.5, 5.1, 4.6 sec) and recognition (Fig. 8c; 3.6, 2.4, 2.8, 2.7 sec) ROIs. All in all, the regions that make up each category deviated little from the average line.

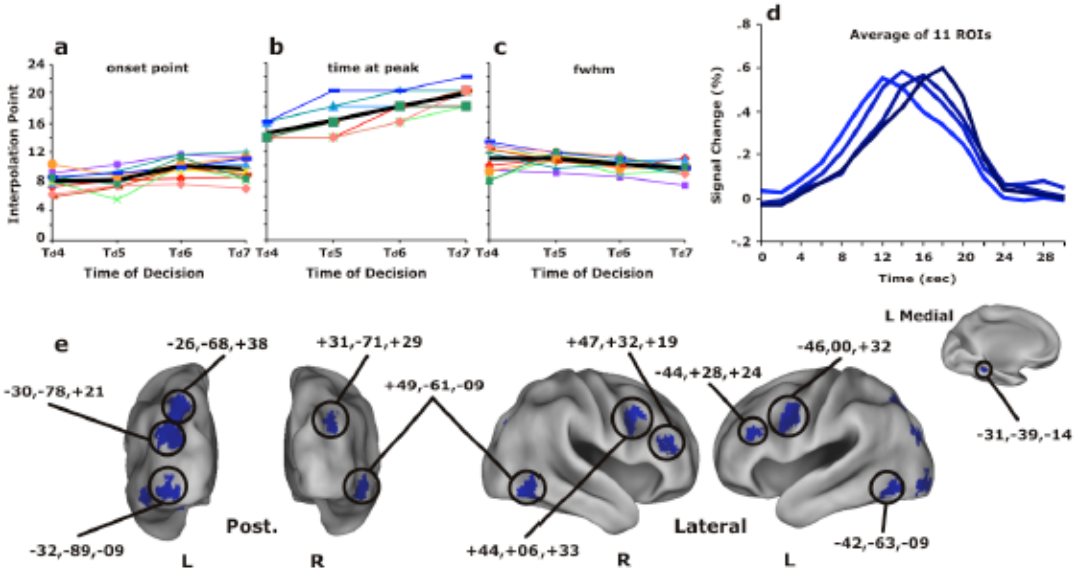

Figure 7. Interpolation analysis, accumulators.

a**) time courses for thirteen accumulator ROIs identified by the interpolation analysis. Time courses are shaded by T_R (see Fig. 4 caption).** b-d) **The data for each accumulator region is shown in blue and the mean of those values is indicated by a thick black line for onset, peak, and width.** e**) ROIs are projected onto posterior and lateral views of inflated cortical surfaces.**

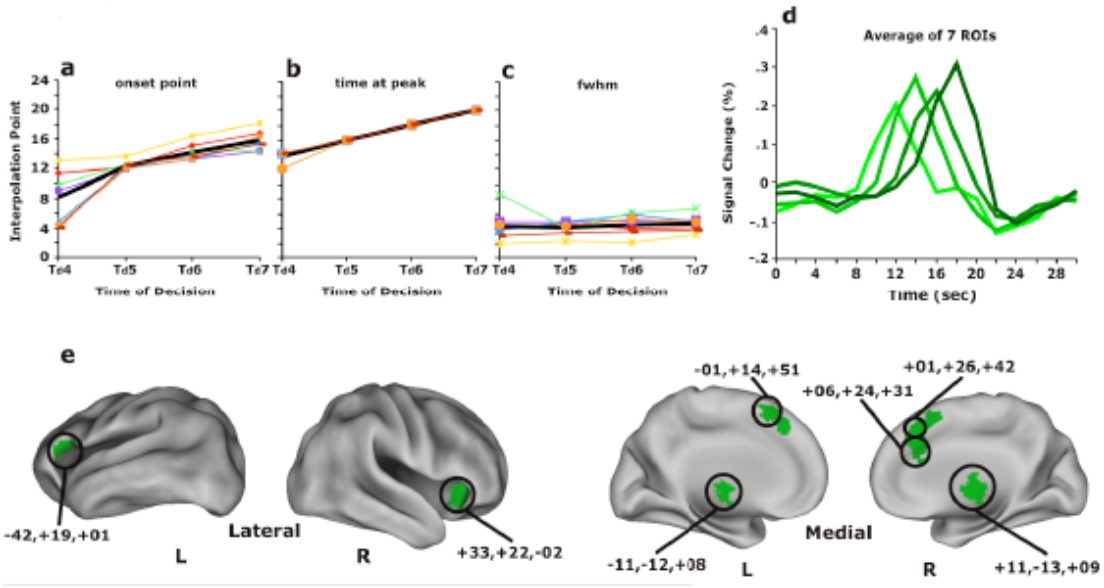

Figure 8. Interpolation analysis, moment of recognition areas.

a**) time courses for fourteen recognition ROIs identified by the interpolation analysis. Time courses are shaded by T_R (see Fig. 4 caption).** b-d) **The data for each recognition region is shown in green and the mean of those values is indicated by a thick black line for onset, peak, and width.** e**) ROIs are projected onto inflated cortical surfaces.**

To test our hypotheses about differences in onset times, peak times, and response width between the three main clusters (i.e., Figs. 6-7a, c), we entered the corresponding values for each ROI into three sets of repeated measures ANOVAs (using SPSS, SPSS, Inc., Chicago, IL) with four levels of the repeated measure T_R (4, 5, 6, 7). In the first analysis in the set, we tested for differences in onset, peak, and width across region grouping by including three levels of the between factor region type (sensory, accumulator, recognition). In the second analysis of the set, when warranted by significant effects in the first, we directly contrasted region groups by including only two levels of the between factor region type and testing each unique combination (sensory, accumulator; sensory, recognition; and accumulator, recognition) in three separate ANOVAs. The second set of analyses investigated the source of significant effects in the first

analysis by making pairwise comparisons of repeated measures models. In the third set we tested the degree to which onset and peak values followed a linear trend across T_R by computing three 1 x 4 repeated measures ANOVAs and including a polynomial trend analysis. In these analyses, the main effect of T_R determines the reliability by which T_R values differ across levels of T_R, while the trend analysis determines whether that change is linear. All F- and p- values of repeated measures incorporate the Greenhouse-Geisser sphericity correction (SPSS) to adjust the degrees of freedom.

Onset Times

The 3 x 4 ANOVA of onset times with the three region groups revealed a significant main effect of T_R ($F[2.5, 73.4] = 14.47$, $p < .0001$) and a significant interaction of T_R with region type ($F[5.1, 73.4] = 10.91$, $p < .0001$), indicating that across regions the onset times differed over levels of T_R, and this effect was modified by region type. The main effect of the between-factor region type was also significant ($F[2, 29] = 31.91$, $p < .0001$). To identify the source of the interaction, we next computed three 2 x 4 ANOVAs on each unique combination of the three ROI types. All three ANOVAs revealed an interaction of region type with T_R (all $p < .05$), indicating that the observed rates of increasing onset values across T_R4-7 (recognition > accumulator > sensory) differed significantly between the three region types.

Next, we computed a separate 1 x 4 repeated measures ANOVA on each region type to determine whether the change in onset times followed a linear trend across levels of T_R. According to these analyses, onset values at different T_Rs did not differ in sensory ROIs ($F[1.3, 5.4] = 1.67$, $p = 0.26$) and did not reliably follow a linear trend across T_R4-7 ($F[1, 4] = 1.04$, $p = 0.37$). In contrast, onset values differed significantly across levels of T_R in accumulator ($F[2.3, 28.1] = 5.93$, $p = .01$) and recognition ($F[2.0, 26.1] = 33.51$, $p < .0001$) ROIs. Both of the latter

region types also showed significant linear trends (accumulator: $F[1, 12] = 13.39$, $p < .0001$; recognition: $F[1, 13] = 75.37$, $p < .0001$), indicating that the onset values increased significantly and linearly as T_R increased.

Combined, the three sets of analyses indicate that onset times increased linearly in accumulator and recognition, but not sensory, ROIs. Furthermore, in accumulator and recognition ROI types, the increase in onset times across levels of T_R differed reliably. Thus, the increasing onset values observed in recognition ROIs was greater than the accumulation ROI values.

Peak Times

To determine whether peak values changed reliably as a function of T_R, we next performed the same set of analyses on interpolated peak times. The 3 x 4 ANOVA with three levels of region type revealed a significant main effect of T_R ($F[2.8, 81.0] = 225.62$, $p < .0001$) and an interaction of T_R with region type ($F[5.6, 81.0] = 8.06$, $p < .0001$), indicating that peak times increased significantly as a function of T_R and that this effect was modified by region type. To explore the source of these differences we next computed three 2 x 4 ANOVAs, each with two levels of region type. In these analyses, interactions of T_R with region type indicated that in sensory ROIs the change in peak values over T_R4-7 differed from accumulator ($F[2.6, 41.1] = 9.64$, $p < .0001$) and recognition ($F[2.2, 38.0] = 17.59$, $p < .0001$) ROIs. However, there was no difference in peak values over T_R4-7 between accumulator and recognition ROIs ($F[2.7, 67.6] = 1.46$, $p = .23$). Thus, increases in time to peak values were greater in accumulator and recognition ROIs than in sensory ROIs. In all three ROI types, the main effect of T_R in the 1 x 4 ANOVAs was significant (all $p < .01$) and all showed a significant linear trend (all $p < .01$). Thus, peak times increased as a function of T_R in all three region types. However, the 2 x 4

analyses indicated that the rate of increase in the sensory ROI group was significantly less than in accumulator and recognition ROI groups.

BOLD Response Width

To test the hypothesis that response widths would be greatest in sensory ROIs, least in recognition ROIs, and intermediate in accumulator ROIs, we first entered the FWHM values into a 3 x 4 ANOVA (describe above). A significant main effect of T_R ($F[2.0, 58.4] = 4.50$, $p < .05$) and a nonsignificant interaction of T_R with region type ($F[4.0, 58.4] = 1.96$, $p = .11$) indicated that width values differed across levels of T_R but not as a function of region type. However, a significant main effect of the between-factor region type ($F[2, 29] = 90.48$, $p < .0001$) revealed a highly reliable difference in widths between regions. Because the interaction was not significant, we did not perform the 2 x 4 regionwise analyses that were conducted on the onset and peak data. Finally, the 1 x 4 ANOVAs revealed no significant main effect of T_R in the sensory ROI group ($F[1.1, 4.3] = 0.32$, $p = .62$), and a significant main effect in the accumulator ($F[1.6, 19.0] = 7.00$, $p < .01$) and recognition ($F[1.5, 19.0] = 4.86$, $p < .05$) ROI groups. Only the accumulator group showed significant linear trends in width values across levels of T_R ($F[1, 12] = 11.41$, $p < .01$. The principle result from this analysis was that response widths, which were greatest for sensory ROIs, least for recognition ROIs, and intermediate for accumulator ROIs, differed significantly across region type.

Slope Analysis

We used the onset and peak times to also determine whether the slopes of the leading edge of BOLD response changed as a function of T_R. Leading edge slopes were computed as follows: $(SC_P – SC_{ON}) / (T_P - T_{ON})$ where SC = percent signal change, T = time

(sec), P = peak, and ON = onset. Specifically, we hypothesized that in accumulators the slope of the leading edge would decrease as decision time increased. To test this hypothesis, we entered slope values from accumulator ROIs (T_R4-7 means: 0.13, 0.11, 0.10, 0.10) into a single factor repeated measures (T_R4-7) ANOVA and included a linear trend analysis to determine whether slope values changed linearly across levels of T_R. This analysis revealed a main effect of T_R ($F[2.1, 25.7] = 6.15$, $p < .01$) and a significant linear trend ($F[1, 12] = 8.91$, $p < .05$). The same analysis on data from recognition ROIs (TR4-7 means: 0.10, 0.13, 0.10, 0.13) revealed neither a main effect of T_R ($F[1.9, 24.6] = 1.28$, $p = 0.29$) nor a significant linear trend ($F[1, 13] = 0.57$, $p = 0.46$).

Atypical responses

While the ROIs clustered into three distinct categories that were broadly consistent with our predicted profiles, some ROIs did not cluster as tightly with the idealized response as others. For example, in two 'accumulator' ROIs located in left cerebellum, and a third ROI in right posterior parietal lobe, activity increased rapidly independently of T_R, but then displayed a more gradual increase that was T_R-dependent. In ROIs located near the right supramarginal gyrus (+34, -57, +47),, right inferior precentral gyrus near frontal operculum (+51, +15, +07) and right posterior inferior frontal gyrus (+45, +14, -03), activity increases were relatively late in the trial, and preceded by a decrease in activity. The late response suggests that these regions may be more involved in processing occurring at VoA than at T_R. As another example, ROIs in or near bilateral striatum (-11, +07, +05; +12, +06, +03), near the head of the caudate nucleus, clustered broadly into the recognition group. However, their timecourse parameters were least similar to other ROIs in the group.

4.0 DISCUSSION

Accurate decision making is a crucial part of survival and operates across modalities, stimulus domains, and cognitive functions. The decision process involves analysis of sensory input, gathering of evidence toward behavioral options, and a later process that allows the selection of a contextually relevant behavior and the evaluation of its appropriateness. We present data indicating that neural mechanisms supporting perceptual recognition decisions can be dissociated using fMRI. These include 1) sensory processors in which activity reflects the quantity of stimulus information entering the system, 2) accumulators that may reflect the gathering of information used to make the decision, and 3) a set of processors that are clearly engaged at, but not before, the time of recognition. Overall, the results help define a hierarchy of neural mechanisms involved in sorting inputs, gathering evidence, and deciding and monitoring an appropriate course of action. In addition, they demonstrate that accumulation processes can be identified using fMRI as dynamically evolving signals.

4.1 SENSORY PROCESSING

During stimulus revelation, activity in posterior occipital regions increased monotonically as a function of the amount of visual information entering the system. Activity in some sensory processors also appeared to vary modestly with T_R, as evidenced by peak latencies that shifted

positively with T_R (Figs 2a, 5). It appears that T_R may have been influenced somewhat by bottom-up stimulus-specific differences in the amount or type of stimulus information available throughout the revelation process. That is, some objects may have been identified earlier in the trial because more critically identifiable features were unmasked earlier. For example, certain visible elements (e.g., geons) provide a higher degree of object level information than straight lines (Biederman, 1987). If true, then T_R-dependent activity in late visual processing areas could have been dependent upon differences in lower level feature extraction in early visual areas. The Exp2 behavioral data support this alternative because recognition times for some items tended to be consistent across subjects (see supplementary text online).

4.2 ACCUMULATION

Regions demonstrating accumulation may compute decision variables, such that the quantity of accrued activity is associated with decision outcome. We found accumulator patterns of response in ROIs in bilateral occipital lobes, fusiform gyrus near LOC (Kourtzi and Kanwisher, 2001), dorsal meFG, dlPFC, and PPL (Fig. 6). The pattern of T_R-dependent accumulation of BOLD activity observed in these regions is consistent with the buildup of neural activity found in studies of non-human primates making perceptual decisions (Hanes and Schall, 1996; Kim and Shadlen, 1999; Platt and Glimcher, 1999; Shadlen and Newsome, 2001; Ratcliff et al., 2003). Interestingly, in an fMRI study with human participants, Kleinschmidt and colleagues (Kleinschmidt et al., 2002) used a perceptual task capable of inducing hysteresis and found right lateralized frontal and parietal, and bilateral occipital/temporal areas in which activity increases were related to a perceptual pop-out effect of letter stimuli. The data are also

reminiscent of a diffusion or random walk process. For example, in Ratcliff's two-choice diffusion model (Ratcliff, 1978; Ratcliff et al., 2004), evidence is accumulated in a drift parameter and decisions are generated when the value of the drift parameter surpasses a response boundary. The level of activity in the accumulator regions may reflect neuronal processing relevant to the recognition decision. When recognition occurred early in the trial, the leading edge of activity followed a steep slope. As recognition time increased, however, the slope became shallower, suggesting a longer diffusion process. Perceptual recognition decisions may occur when activity in one or more accumulators surpasses a response threshold. Because we could not perform trial-level analyses, the findings are not specific enough to test different accounts of accumulator model. We note the relationship instead to build a conceptual link between the current findings and theoretical accounts of decision making.

It seems plausible that component processes related to analysis of visual features and semantic knowledge could contribute to a pattern of accumulation. Thus, the degree to which the T_R-dependent buildup in activity reflects 'evidence accumulation' *per se* is not clear. For example, it is plausible that accumulating activity is a mere byproduct of information processing rather than an informative mechanism. According to this view, the level of activity does not reflect the integration of information over time, but is instead perhaps a consequence of the timing by which neurons are recruited. In our view, the tight coupling of the rate of activity buildup and T_R in our data and in single unit studies in non-human primates (Kim and Shadlen, 1999; Shadlen and Newsome, 2001) suggests that a purely epiphenomenal account is unlikely. However, further experiments are needed to test the content- and task-specificity of accumulation to the decision making process.

It is worth noting that some parietal regions displaying accumulation responses

are near parietal ‘retrieval success’ regions identified in episodic memory studies using old/new recognition and source memory tasks (Habib and Lepage, 1999; Konishi et al., 2000; McDermott et al., 2000; Donaldson et al., 2001a; Donaldson et al., 2001b; Wheeler and Buckner, 2003, 2004). For example, regions near the IPS (e.g., -26, -68, 38) and precuneus (-9, -56, 34) demonstrated an accumulator pattern of responses. Several studies of recognition memory have reported that IPS and precuneus are most active when participants respond “old” and least active when they respond “new”, independently of accuracy (Wheeler and Buckner, 2003; Kahn et al., 2004). The association between the decision outcome and level of BOLD signal suggests that the memory decision may have been based on a simple threshold process. This finding has raised the possibility that the function of such regions is to accumulate and maintain relevant mnemonic information over time in memory tasks. The current data show that activity in IPS and precuneus gradually accumulates until the moment of recognition, and thus suggest a more domain-general integrative mechanism supporting episodic recognition and perceptual identification.

4.3 RECOGNITION DECISION

Activity in a small set of regions, including bilateral thalamus, meFG/pre-SMA, dorsal ACC, and aI/fO was tightly coupled to the time of recognition (Fig. 7). The precise role of meFG / pre-SMA (which is sometimes referred to as dACC) is unclear, though its function does not appear to be directly related to action planning or execution (Picard and Strick, 2001). The absence of a clear response at VoA supports this view because the motor demand at that stage of the trial did not produce a marked change in signal. In contrast, in motor ROIs we observed a transient change in BOLD signal at both recognition and VoA. The ACC, and more recently the

aI/fO, have both been associated with aspects of decision making, including choice (Hampton and O'Doherty, 2007; Thielscher and Pessoa, 2007), error detection (Dehaene et al., 1994), error likelihood (Brown and Braver, 2005), reward evaluation (Rogers et al., 1999; Sanfey et al., 2003), attention for action (Posner et al., 1988; Posner and Petersen, 1990; Bush et al., 1998), response conflict/competition (Bush et al., 1998; Botvinick et al., 1999; Botvinick et al., 2001), confidence (Fleck et al., 2006), and uncertainty (Grinband et al., 2006). The current results do not directly differentiate among these possibilities, but do temporally dissociate processes occurring at the moment of recognition and the subsequent verification of that recognition.

The current work extends previous research findings by demonstrating that regions in pre-SMA, ACC, aI/fO, and thalamus show strong activity to cognitive events that arise at, but not before, the moment of recognition. For example, decisions were made at the time of recognition and again at VoA. If these ROIs were obligatorily involved in decision making, then we would expect a bimodal time course, the first peak time-locked with T_R and the second associated with VoA (see Figs. 4d). Instead, it appears that activity in areas recruited at the moment of recognition reflects contingencies regarding their recruitment; these regions were clearly more involved at the time of recognition than at the time of verification. Alternatively, if these ROIs perform a monitoring function on information processing prior to a decision, then we would expect to see signal modulations prior to T_R. This was clearly not the case. Further, it has been hypothesized that several of these regions play a role in error detection (Dehaene et al., 1994). Though we did not present the error data due to space constraints, error trials were associated with significantly greater T_R-dependent activity in the moment of recognition ROIs than correct trials. However, a pure error detection hypothesis is not supported by the current data because T_R-dependent BOLD responses were clearly evident on correct trials as well.

Instead, errors appear to modulate other processing occurring in these areas.

4.4 SUMMARY

The overall pattern of data suggests a hierarchical framework of neural mechanisms that are recruited during decision making. In this framework, information processing proceeds through sensory processing and evidence accumulation to decision mechanisms, and culminates in a behavior. Presumably, this process begins with the task-level assignment of setting decision criteria and includes post-decision monitoring. The precise functional relationship between accumulators and moment-of-recognition areas remains unclear. For example, it is unclear whether decisions arise from processing in accumulators or in regions active at the moment of recognition (or elsewhere). Future research on task-specificity may be informative in determining if and how accumulating information is interpreted by decision mechanisms, whether they are task-specific or task-general, and how decisions are reached and enacted.

Table 1. Peak locations and coordinates for ROIs belonging to the negative waveform cluster

Anatomic Location	~BA	X	Y	Z
L Paracentral Lobule (1)	6	-1	-32	58
R Middle Frontal Gyrus (2)	6	24	-7	59
R Posterior Cingulate (3)	31	15	-43	40
R Superior Temporal Gyrus (4)	41	38	-34	17
R Superior Temporal Gyrus (5)	22	57	-8	7
R Superior Temporal Gyrus (6)	42	54	-31	15
R Posterior Insula (7)	13	47	-18	15
L Superior Temporal Gyrus (8)	41	-55	-20	8
L Posterior Insula (9)	13	-39	-21	12
L Superior Temporal Gyrus (10)	42	-55	-33	11
L Superior Temporal Gyrus (11)	41	-42	-36	11
R Precuneus (12)	7	11	-46	51
L Middle Temporal Gyrus (13)	39	-51	-62	27
R Superior Parietal Lobule (14)	7	28	-47	61
L Posterior Cingulate (15)	31	-14	-39	39
L Precuneus (16)	31	-9	-56	34
R Precuneus (17)	7	8	-52	61
L Precuneus (18)	7	-12	-47	51
L Precuneus (19)	7	-8	-61	61
L Precuneus (20)	7	-1	-46	56
R Anterior Cingulate (21)	32	4	46	-03
R Cingulate Gyrus (22)	31	7	-47	27

Anatomic Location	~BA	X	Y	Z
L Precuneus (23)	7	-1	-59	53
R Precuneus (4d) (24)	7	2	-60	37

Notes. L = left; R = right; ~BA = approximate Brodmann's area; X, Y, Z = atlas coordinate dimensions; ROI order follows cluster tree displayed in Fig. 4. Anatomic locations are approximate.

Table 2. Peak locations and coordinates for ROIs belonging to the late positive waveform cluster

Anatomic Location	~BA	X	Y	Z
R Cuneus (25)	18	14	-82	28
L Cuneus (4c) (26)	18	-1	-83	25
R Parahippocampal Gyrus (27)	19	17	-52	-4
L Lingual Gyrus (28)	19	-16	-57	-2
L Lingual Gyrus (29)	18	-9	-68	2
R Cuneus (30)	30	11	-69	10
L Cuneus (31)	17	-5	-77	13

Notes. L = left; R = right; ~BA = approximate Brodmann's area; X, Y, Z = atlas coordinate dimensions; ROI order follows cluster tree displayed in Fig. 3. Anatomic locations are approximate.

Table 3. Peak locations and coordinates for ROIs belonging to the bimodal waveform cluster

Anatomic Location	~BA	X	Y	Z
L Anterior Cingulate (32)	32/24	-10	35	14
L Posterior Parietal Lobe (33)	7	-28	-44	51
L Postcentral Gyrus (34)	43	-49	-11	16
L Cingulate Gyrus (35)	24	0	10	31
L Middle Temporal Gyrus (36)	39	-42	-74	13
L Cingulate Gyrus (37)	24	-10	4	39
L Cingulate Gyrus (38)	32	-9	28	27
R Anterior Cingulate (39)	32	9	32	25
R Cerebellum (40)		11	-71	-23
L Middle Frontal Gyrus (41)	6	-25	-10	55

Notes. L = left; R = right; ~BA = approximate Brodmann's area; X, Y, Z = atlas coordinate dimensions; ROI order follows cluster tree displayed in Fig. 3. Anatomic locations are approximate.

Table 4. Peak locations, coordinates, and interpolation group for ROIs belonging to the positive waveform cluster

Anatomic Location	~BA	X	Y	Z	Interpolation Group
R Precentral Gyrus (42)	44	51	15	07	Moment of recognition
R Inferior Frontal Gyrus (43)	47	45	14	-03	Moment of recognition
R Inferior Parietal Lobule (44)	40	49	-48	47	Moment of recognition
R Medial Frontal Gyrus (45)	8	01	26	42	Moment of recognition
L Medial Frontal Gyrus (4e) (46)	6	-01	14	51	Moment of recognition

Anatomic Location	~BA	X	Y	Z	Interpolation Group
R Anterior Cingulate (47)	32	06	24	31	Moment of recognition
L Thalamus (48)		-11	-12	08	Moment of recognition
R Thalamus** (49)		11	-13	09	Moment of recognition
L Striatum (50)		-11	07	05	Moment of recognition
R Striatum (51)		12	06	03	Moment of recognition
L Inferior Frontal Gyrus (52)	47	-42	19	01	Moment of recognition
R Anterior Insula (4f) (53)	13	33	22	-02	Moment of recognition
L Anterior Insula (54)	13	-32	22	01	Moment of recognition
R Inferior Parietal Lobule (55)	7	34	-57	47	Moment of recognition
L Cerebellum (56)		-26	-79	-22	Accumulator
L Cerebellum (57)		-34	-72	-27	Accumulator
L Middle Frontal Gyrus* (58)	46	-44	28	24	Accumulator
L Fusiform Gyrus (59)	20	-31	-39	-14	Accumulator
L Inferior Occipital Gyrus (60)	18	-32	-89	-09	Accumulator
R Fusiform Gyrus** (61)	37	49	-61	-09	Accumulator
R Middle Frontal Gyrus** (62)	46	47	32	19	Accumulator
L Intraparietal Sulcus (63)	7/19	-26	-68	38	Accumulator
L Fusiform Gyrus (4b)** (64)	37	-42	-63	-09	Accumulator
R Inferior Frontal Gyrus (65)	6/9	44	06	33	Accumulator
R Middle Occipital Gyrus (66)	19	30	-78	17	Accumulator
L Middle Occipital Gyrus* (67)	19	-30	-78	21	Accumulator
R Superior Occipital Gyrus** (68)	19/39	31	-71	29	Accumulator

Anatomic Location	~BA	X	Y	Z	Interpolation Group
L Posterior Inf. Frontal Gyrus** (69)	9/6	-46	0	32	Accumulator
R Lingual Gyrus (70)	17	01	-93	-06	Sensory Processor
L Cuneus (4a) (71)	18	-19	-99	02	Sensory Processor
L Lingual Gyrus (72)	18	-10	-99	-05	Sensory Processor
R Cuneus (73)	18	16	-99	-01	Sensory Processor

Notes. L = left; R = right; ~BA = approximate Brodmann's area; X, Y, Z = atlas coordinate dimensions; ROI order follows cluster tree displayed in Fig. 3. Anatomic locations are approximate.

BIBLIOGRAPHY

Attwell, D. & Iadecola, C. (2002). The neural basis of functional brain imaging signals. *TRENDS In Neurosciences,* 25(12):621-625.

Audley RJ, Pike AR (1965) Some stochastic models of choice. British Journal of Mathematical and Statistical Psychology 18:183-192.

Awh, E. & Jonides, J. (1998). Spatial working memory and spatial selective attention. In: Parasuraman, R. (Ed.), The Attentive Brain. MIT Press.

Biederman I (1987) Recognition-by-components: A theory of human image understanding. Psychological Review 94:115-147.

Botvinick M, Nystrom LE, Fissell K, Carter CS, Cohen JD (1999) Conflict monitoring versus selection-for-action in anterior cingulate cortex. Nature 402:179-181.

Botvinick MM, Braver TS, Barch DM, Carter CS, Cohen JD (2001) Conflict monitoring and cognitive control. Psychological Review 108:624-652.

Boynton GM, Engel SA, Glover GH, Heeger DJ (1996) Linear systems analysis of functional magnetic resonance imaging in human V1. Journal of Neuroscience 16:4207-4221.

Brown, A.S. (1991). A review of the tip-of-the-tongue experience. *Psychological Bulletin,* 109(2):204-223.

Brown JW, Braver TS (2005) Learned predictions of error likelihood in the anterior cingulate cortex.[see comment]. Science 307:1118-1121.

Bundesen C (1990) A theory of visual attention. Psychological Review 97:523-547.

Busemeyer J (1985) Decision making under uncertainty: A comparison of simple scalability, fixed-sample, and sequential-sampling models. Journal of Experimental Psychology: Learning, Memory, and Cognition 11:538-564.

Bush G, Whalen PJ, Rosen BR, Jenike MA, McInerney SC, Rauch SL (1998) The Counting Stroop: An interference task specialized for functional neuroimaging: Validation study with functional MRI. Human Brain Mapping 6:270-282.

Bush G, Vogt BA, Holmes J, Dale AM, Greve D, Jenike MA, Rosen BR (2002) Dorsal anterior cingulate cortex: a role in reward-based decision making. Proceedings of the National Academy of Sciences of the United States of America 99:523-528.

Carlson T, Grol MJ, Verstraten FA (2006) Dynamics of visual recognition revealed by fMRI. Neuroimage 32:892-905.

Cohen, G. & Faulkner, D. (1986). Memory for proper names: Age differences in retrieval. *British Journal of Developmental Psychology*, 4:187-197.

Cohen JD, MacWhinney B, Flatt M, Provost J (1993) PsyScope: A new graphic interactive environment for designing psychology experiments. Behavioral Research Methods, Instruments, and Computers 25:257-271.

Cook EP, Maunsell JH (2002) Dynamics of neuronal responses in macaque MT and VIP during motion detection. Nature Neuroscience 5:985-994.

Cordes D, Haughton V, Carew JD, Arfanakis K, Maravilla K (2002) Hierarchical clustering to measure connectivity in fMRI resting-state data. Magnetic Resonance Imaging 20:305-317.

Dale & Buckner, R. (1997). Selective averaging of rapidly presented individual trials using fMRI. *Human Brain Mapping,* 5:329-340.

Dehaene S, Posner M, Tucker D (1994) Localization of a neural system for error detection and compensation. Psychological Science 5:303-305.

Donaldson DI, Petersen SE, Buckner RL (2001a) Dissociating memory retrieval processes using fMRI: Evidence that priming does not support recognition memory. Neuron 31:1047-1059.

Donaldson DI, Petersen SE, Ollinger JM, Buckner RL (2001b) Dissociating state and item components of recognition memory using fMRI. Neuroimage 13:129-142.

Dosenbach N, Fair D, Miezin F, Cohen A, Wenger K, Dosenbach R, Fox M, Snyder A, Vincent J, Raichle M, Schlaggar B, Petersen S (2007) Distinct brain networks for adaptive and stable task control in humans. Proceedings of the National Academy of Sciences of the United States of America 104:11073-11078.

Everitt, B. (1993). Cluster analysis, 3rd edition. Halsted Press, London.

Fleck MS, Daselaar SM, Dobbins IG, Cabeza R (2006) Role of prefrontal and anterior cingulate regions in decision-making processes shared by memory and nonmemory tasks. Cerebral Cortex 16:1623-1630.

Fox MD, Snyder AZ, Barch DM, Gusnard DA, Raichle ME (2005) Transient BOLD responses at block transitions. Neuroimage 28:956-966.

Frederiksen & Kroll (1976). Spelling and sound: approaches to the internal lexicon. *Journal of Experimental Psychology: Human Perception and Performance*, 2(3):361-379.

Friston, K.J. (1999). Stochastic designs in event-related fMRI. *NeuroImage*, 10:607-619.

Friston K, Jezzard P, Turner R (1994) Analysis of functional MRI time-series. Human Brain Mapping 1:153-171.

Gold, J. & Shadlen, M.N. (2001). Neural computations that underlie decisions about sensory stimuli. *TRENDS in Cognitive Sciences*, 5(1):10-16.

Gold J, Shadlen M (2007) The neural basis of decision making. Annual Review of Neuroscience 30:535-574.

Grinband J, Hirsch J, Ferrera V (2006) A neural representation of categorization uncertainty in the human brain. Neuron 49:757-763.

Habib R, Lepage M (1999) Novelty assessment in the brain. In: Memory, Consciousness, and the Brain (Tulving E, ed), pp 265-277. Philadelphia, PA: Psychology Press.

Hampton AN, O'Doherty JP (2007) Decoding the neural substrates of reward-related decision making with functional MRI. Proceedings of the National Academy of Sciences of the United States of America 104:1377-1382.

Handl J, Knowles J, Kell D (2005) Computational cluster validation in post-genomic data analysis. Bioinformatics 21:3201-3212.

Hanes DP, Schall JD (1996) Neural control of voluntary movement initiation. Science 274:427-430.

Hanks TD, Ditterich J, Shadlen MN (2006) Microstimulation of macaque area LIP affects decision-making in a motion discrimination task. Nature Neuroscience 9:682-689.

Heekeren HR, Marrett S, Bandettini PA, Ungerleider LG (2004) A general mechanism for perceptual decision-making in the human brain. Nature 431:859-862.

Hernandez (2000). Neuronal correlates of sensory discrimination in the somatosensory cortex. *PNAS*, 97:6191-6196.

Hockley, W.E. & Murdock, B.B. (1987). A decision model for accuracy and response latency in recognition memory. *Psychological Review*, 94:341-358.

Huk & Shadlen, M.N. (2005). Neural activity in macaque parietal cortex reflects temporal integration of visual motion signals during perceptual decision making. *Journal of Neuroscience*, 25(45):10420-10436.

James T, Humphrey G, Gati J, Menon R, Goodale M (2000) The effects of visual object priming on brain activation before and after recognition. Current Biology 10:1017-1024.

Jung-Beeman, M. et al (2004). Neural activity when people solve verbal problem with insight. *PLoS Biology*, 2(4):500-510.

Kahn I, Davachi L, Wagner AD (2004) Functional-neuroanatomic correlates of recollection: implications for models of recognition memory. J Neurosci 24:4172-4180.

Kim J-N, Shadlen MN (1999) Neural correlates of a decision in the dorsolateral prefrontal cortex of the macaque. Nature Neuroscience 2:176-185.

Kinchla, R.A. & Smyzer, F. (1967.) A diffusion model of perceptual memory. *Perception & Psychophysics*, 2:219-229.

Kleinschmidt A, Buchel C, Hutton C, Friston KJ, Frackowiak RS (2002) The neural structures expressing perceptual hysteresis in visual letter recognition.[see comment]. Neuron 34:659-666.

Konishi S, Wheeler ME, Donaldson DI, Buckner RL (2000) Neural correlates of episodic retrieval success. Neuroimage 12:276-286.

Koriat, A. & Leiblich, I. (1977). A study of memory pointers. *Acta Psychologica*, 41:151-164.

Kourtzi Z, Kanwisher N (2001) Representation of perceived object shape by the human lateral occipital complex. Science 293:1506-1509.

Kwong, K.K., et al (1992). Dynamic magnetic resonance imaging of human brain activity during primary sensory stimulation. *PNAS*, 89:5675-5679.

Lancaster JL, Glass TG, Lankipalli BR, Downs H, Mayberg H, Fox PT (1995) A modality-independent approach to spatial normalization of tomographic images of the human brain. Human Brain Mapping 3:209-223.

Levy I, Hasson U, Avidan G, Hendler T, Malach R (2001) Center-periphery organization of human object areas. Nature Neuroscience 4:533-539.

Link S, Heath R (1975) A sequential theory of psychological discriminations. Psychometrika 40:77-105.

Logan GD, Gordon RD (2001) Executive control of visual attention in dual-task situations. Psychological Review 108:393-434.

Logothetis, N., et al (2001). Neurophysiological investigation of the basis of the fMRI signal. *Nature*, 412:150-157.

Maril, A., Wagner, A.D., and Schacter, D.L. (2001). On the tip-of-the-tongue: An event-related fMRI study of semantic retrieval failure and cognitive conflict. *Neuron*, 31:653-660.

Mazurek, M.E., et al (2003). A role for neural integrators in perceptual decision making. *Cerebral Cortex*, 13:1257-1269.

McAvoy MP, Ollinger JM, Buckner RL (2001) Cluster size thresholds for assessment of significant activation in fMRI. NeuroImage 13:S198.

McDermott KB, Jones TC, Petersen SE, Lageman SK, Roediger III HL (2000) Retrieval success is accompanied by enhanced activation in anterior prefrontal cortex during recognition memory: An event-related fMRI study. Journal of Cognitive Neuroscience 12:965-976.

McKeeff, T.J. & Tong, F. (2007). The timing of perceptual decisions for ambiguous face stimuli in the human ventral visual cortex. *Cerebral Cortex*, 17:669-678.

Metcalfe, J. (1986). Feeling of knowing in memory and problem-solving. *Journal of Experimental Psychology: Learning, Memory, and Cognition*, 12(2):288-294.

Metcalfe, J. & Weibe, D. (1987). Intuition in insight and noninsight problem solving. *Memory & Cognition*, 15:238-246.

Michelon P, Snyder AZ, Buckner RL, McAvoy M, Zacks JM (2003) Neural correlates of incongruous visual information. An event-related fMRI study. Neuroimage 19:1612-1626.

Miezin F, Maccotta L, Ollinger J, Petersen S, Buckner R (2000) Characterizing the hemodynamic response: Effects of presentation rate, sampling procedure, and the possibility of ordering brain activity based on relative timing. NeuroImage 11:735-759.

Nosofsky R, Palmeri T (1997) An exemplar-based random walk model of speeded classification. Psychological Review 104:266-300.

Ogawa, S., Lee, T.M., Kay, A.R., and Tank, D.W. (1990). Brain magnetic resonance imaging with contrast dependent on blood oxygenation. *PNAS*, 87:9868-9872.

Ogawa, S., et al (1992). Intrinsic signal changes accompanying sensory stimulation: functional brain mapping with magnetic resonance imaging. *PNAS*, 89:5951-5955.

Ojemann JG, Akbudak E, Snyder AZ, McKinstry RC, Raichle ME, Conturo TE (1997) Anatomic localization and quantitative analysis of gradient refocused echo-planar fMRI susceptibility artifacts. Neuroimage 6:156-167.

Ollinger JM, Shulman GL, Corbetta M (2001) Separating processes within a trial in event-related functional MRI I. The method. Neuroimage 13:210-217.

Palmer, J., Huk, A.C., and Shadlen, M.N. (2005). The effect of stimulus strength on the speed and accuracy of a perceptual decision. *Journal of Vision*, 5:376-404.

Picard N, Strick P (2001) Imaging the premotor areas. Current Opinion in Neurobiology 11:663-672.

Platt ML, Glimcher PW (1999) Neural correlates of decision variables in parietal cortex. Nature 400:233-238.

Ploran EP, Nelson SMM, Donaldson DI, Petersen SE, Wheeler ME (2006) Evidence accumulation and the moment of recognition: an exploration of decision processes using fMRI. In: Society for Neuroscience. Atlanta, GA.

Posner MI, Petersen SE (1990) The attention system of the human brain. Annual Review of Neuroscience 13:25-42.

Posner MI, Petersen SE, Fox PT, Raichle ME (1988) Localization of cognitive operations in the human brain. Science 240:1627-1631.

Pruett, J.R., Sinclair, R.J., and Burton, H. (2001). Neural correlates for roughness choice in monkey second somatosensory cortex (SII). *Journal of Neurophysiology*, 86:2069-2080.

Ratcliff R (1978) A theory of memory retrieval. Psychological Review 85:59-108.

Ratcliff, R. (2002). A diffusion model account of response time and accuracy in a brightness discrimination task: fitting real data and failing to fit fake but plausible data. *Psychonomic Bulletin & Review*, 9(2):278-291.

Ratcliff R, McKoon G (1982) Speed and accuracy in the processing of false statements about semantic information. Journal of Experimental Psychology: Learning, Memory, and Cognition 8:16-36.

Ratcliff R, Rouder JN (1998) Modeling response times for two-choice decisions. Psychological Science 9:347-356.

Ratcliff R, Cherian A, Segraves M (2003) A comparison of macaque behavior and superior colliculus neuronal activity to predictions from models of two-choice decisions. Journal of Neurophysiology 90:1392-1407.

Ratcliff R, Gomez P, McKoon G (2004) A Diffusion Model Account of the Lexical Decision Task. Psychological Review 111:159-182.

Rogers RD, Owen AM, Middleton HC, Williams EJ, Pickard JD, Sahakian BJ, Robbins TW (1999) Choosing between small, likely rewards and large, unlikely rewards activates inferior and orbital prefrontal cortex. Journal of Neuroscience 19:9029-9038.

Roitman JD, Shadlen MN (2002) Response of neurons in the lateral intraparietal area during a combined visual discrimination reaction time task. Journal of Neuroscience 22:9475-9489.

Romesburg, H.C. (1984). Cluster analysis for researchers. Lifetime Learning Publications, Belmont, CA.

Romo, R. & Salinas, E. (2003). Flutter discrimination: neural codes, perception, memory and decision making. *Nature Reviews: Neuroscience*, 4:203-218.

Rossion B, Pourtois G (2004) Revisiting Snodgrass and Vanderwart's object pictorial set: The role of surface detail in basic-level object recognition. Perception 33:217-236.

Rubin, D.C. (1975). Within word structure in the tip-of-the-tongue phenomenon. *Journal of Verbal Learning and Verbal Behavior*, 14:392-397.

Salinas, E., Hernandez, A., Zainos, A., and Romo, R. (2000). Periodicity and firing rate as candidate neural codes for the frequency of vibrotactile stimuli. *Journal of Neuroscience*, 20(14):5503-5515.

Salvador R, Suckling J, Coleman MR, Pickard JD, Menon D, Bullmore E (2005) Neurophysiological architecture of functional magnetic resonance images of human brain. Cerebral Cortex 15:1332-1342.

Sanfey AG, Rilling JK, Aronson JA, Nystrom LE, Cohen JD (2003) The neural basis of economic decision-making in the Ultimatum Game.[see comment]. Science 300:1755-1758.

Schlaggar BL, Brown TT, Lugar HM, Visscher KM, Miezin FM, Petersen SE (2002) Functional neuroanatomical differences between adults and school-age children in the processing of single words. Science 296:1476-1479.

Shadlen, M.N. & Gold, J. (2004). The neurophysiology of decision making as a window into cognition. In: Gazzaniga, M.S. (Ed.), The Cognitive Neurosciences, 3rd edition. MIT Press.

Shadlen MN, Newsome WT (2001) Neural basis of a perceptual decision in the parietal cortex (area LIP) of the rhesus monkey. Journal of Neurophysiology 86:1916-1936.

Smith PL, Vickers D (1988) The accumulator model of two-choice discrimination. Journal of Mathematical Psychology 32:135-168.

Snyder AZ (1996) Difference image versus ratio image error function forms in PET-PET realignment. In: Quantification of brain function using PET (Bailey D, Jones T, eds). San Diego: Academic Press.

Talairach J, Tournoux P (1988) Co-Planar Stereotaxic Atlas of the Human Brain. New York: Thieme Medical Publishers, Inc.

Thielscher A, Pessoa L (2007) Neural correlates of perceptual choice and decision making during fear-disgust discrimination. Journal of Neuroscience 27:2908-2917.

Usher M, McClelland JL (2001) The time course of perceptual choice: The leaky, competing accumulator model. Psychological Review 108:550-592.

Wheeler M, Shulman G, Buckner R, Miezin F, Velanova K, Petersen S (2006) Evidence for separate perceptual reactivation and search processing during remembering. Cerebral Cortex 16:949-959.

Wheeler ME, Buckner RL (2003) Functional dissociation among components of remembering: Control, perceived oldness, and content. Journal of Neuroscience 23:3869-3880.

Wheeler ME, Buckner RL (2004) Functional-anatomic correlates of remembering and knowing. Neuroimage 21:1337-1349.

Winer B, Brown D, Michels K (1991) Statistical Principles in Experimental Design, Third Edition. New York: McGraw-Hill.